Computers & Operations Research 189 (2026) 107390

Contents lists available at ScienceDirect

Computers and Operations Research

journal homepage: www.elsevier.com/locate/cor

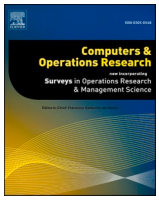

Humanitarian relief logistics network design considering facility location, inventory pre-positioning and evacuation planning: A two-stage distributionally robust optimization approach

Tao Zhang [a,b], Shuaian Wang [c], Xu Xin [a,c,*]

[a] School of Economics and Management, Tongji University, Shanghai 200092, PR China
[b] Department of Industrial and Systems Engineering, Faculty of Engineering, The Hong Kong Polytechnic University, Hung Hom, Hong Kong, PR China
[c] Department of Logistics and Maritime Studies, Faculty of Business, The Hong Kong Polytechnic University, Hung Hom, Hong Kong, PR China

ARTICLE INFO

Keywords:
Emergency facility location
Relief inventory pre-positioning
Evacuation planning
Type-1 Wasserstein metric
Distributionally robust optimization
Benders-decomposition

ABSTRACT

The high uncertainty in the occurrence, space, and scale of natural disasters presents significant challenges to reliable humanitarian relief logistics network (HRLN) design. After a disaster occurs, relief supplies and evacuees are usually transported simultaneously through the HRLN, which occupies limited logistics infrastructure (i.e., roads). This phenomenon drives the integration of three crucial decisions in the design of HRLNs: the emergency facility locations, the pre-positioning of the relief inventory, and the human evacuation planning. This composite problem is formulated as a two-stage distributionally robust optimization model, with the two stages corresponding to pre-disaster and post-disaster decision-making. To capture the characteristics of the distribution functions of the number of evacuees and the road capacity, we design an ambiguity set using historical data and the type-1 Wasserstein metric. We show that there is an equivalent reformulation of the abovementioned model that can be solved by decomposition algorithms. Two versions of the decomposition algorithm, i.e., single-cut and multi-cut versions, are developed based on the generic Benders-decomposition technique. A case study is conducted on the Yushu earthquake in China and several managerial implications are proposed.

1. Introduction

In recent years, both the severity and number of natural disasters that pose a direct threat to humans have clearly increased (Wang et al., 2024). Natural disasters (e.g., earthquakes, tropical storms, hurricanes, tsunamis, and floods) have resulted in millions of casualties and significant economic losses (Zhang et al., 2023). For instance, it is estimated that approximately twice every three years, a major hurricane makes landfall on the Gulf of Mexico or the Atlantic coast of the US, resulting in significant economic losses (El Tonbari et al., 2024). The 2018 Wenchuan earthquake in China's Sichuan Province had a magnitude of M_w 8.0 (Fan et al., 2018), resulting in 69,227 deaths and 17,923 individuals reported missing. Between 2019 and 2021, all types of major natural disasters affected 127 countries and regions, resulting in 27,268 deaths and a direct economic loss of USD 547,171 million (Yin et al., 2024b). In this context, a rapid response to a disaster event undoubtedly contributes to reducing casualties and effectively minimizing the devastating effects of a disaster (Fan et al., 2018). For example, while the survival rate was 91 % within 30 min of the earthquake, it subsequently declined to 81 % on the first day after the earthquake. This figure decreased to 37 % on the second day (Recchiuto & Sgorbissa, 2018). Thus, it is not surprising that various government and non-governmental organizations around the globe have made considerable investments in resources to establish humanitarian relief logistics networks (HRLNs). Nevertheless, how to design effective and reliable HRLNs in disaster environments has always been a challenging task for the academic community and (non)government departments.

In the aforementioned HRLN, two types of flows exist and flow simultaneously: (1) *relief supply flow* and (2) *evacuee flow*. A stable relief supply flow is a prerequisite for implementing post-disaster relief operations, and these supplies are usually stored in emergency facilities (Liu et al., 2025; Wang et al., 2024). If emergency facilities (e.g.,

* Corresponding author at: School of Economics and Management, Tongji University, Shanghai 200092, PR China.
E-mail addresses: taozhang@tongji.edu.cn, tao-zt.zhang@connect.polyu.hk (T. Zhang), hans.wang@polyu.edu.hk (S. Wang), xu-david.xin@connect.polyu.hk, xinxu@tongji.edu.cn (X. Xin).
URL: https://xinxu.space/xinxu-en/ (X. Xin).

https://doi.org/10.1016/j.cor.2026.107390
Received 21 January 2025; Received in revised form 21 September 2025; Accepted 9 January 2026
Available online 14 January 2026

distribution centers, rescue shelters) are located close to the disaster site, then the relief supplies in the facilities can be transported to the disaster area more quickly, making relief operations easier (Zhang et al., 2023). However, the occurrence of disasters is unpredictable in both time and location and cannot be predicted until a disaster actually occurs (El Tonbari et al., 2024). Thus, before a disaster occurs, the decision maker (e.g., the government) must make two strategic decisions: the location and scale of facilities such as rescue shelters and distribution centers, and the location and quantity of relief supplies (e.g., food, basic medicine, tents, and drinking water) to be pre-positioned. After a disaster strikes, pre-positioned relief supplies are transported in the HRLN (usually from the facility to the affected area or transferred between facilities; see Jin et al. (2024)). This type of problem is defined by the term emergency **F**acility **L**ocation and relief supply **I**nventory **P**re-positioning (FLIP). Notably, the population also needs to move through the HRLN (Yin et al., 2024a). According to Salmerón and Apte (2010), the disaster-affected population can be divided into two categories: the *stay-back population*, which includes individuals who are able to remain in the affected area but require the provision of relief supplies to ensure their survival; and the *transfer population* (i.e., evacuee), which comprises individuals in need of emergency medical evacuation and those who are vulnerable to the effects of secondary disasters and require evacuation. The movement of the latter within the HRLN constitutes the evacuee flow. Therefore, in the post-disaster stage, decision makers must also consider developing an evacuation plan to achieve the rational flow (evacuation) of evacuees in the HRLN, which is referred to as the **H**uman **E**vacuation **P**lanning problem (HEP). When designing HRLNs, it is essential to consider both types of flows through the HRLN (Yin et al., 2024a). This is because as evacuees move through the HRLN, the demand for relief supply in each disaster area also changes simultaneously.

Moreover, the unpredictable nature of disasters presents a challenge for decision makers in obtaining complete and accurate information (Wang et al., 2024). Therefore, the primary challenge in establishing an effective HRLN is the inherent uncertainty that exists. On the one hand, the *number of evacuees* generated is uncertain. Owing to the different scales of each disaster, there is uncertainty about the number of people who need to be evacuated, which further creates uncertainty associated with the quantity of relief supplies needed at each disaster area and rescue shelter. Even in the same region, disasters occurring at different times can result in different numbers of disaster areas and numbers of evacuees. On the other hand, although the majority of the literature assumes that the HRLN remains intact and operational following a disaster, this is unlikely to be the case (Zhang et al., 2023). For instance, after the Haiti earthquake on January 12, 2010, damaged roads and the inability to carry out logistics meant that affected people could not obtain enough relief supplies, which ultimately led to the death of 222,500 people (Chu & Chen, 2016). Another example is the earthquake and subsequent tsunami in Japan in April 2011, which caused damage to railways, highways and various logistics hubs. After the disaster, the region's highways were severely damaged, with nearly 76 % of them closed. This significantly impedes emergency rescue activities (Kazama & Noda, 2012). Moreover, in discussing the aforementioned two problems (i.e., FLIP and HEP), it becomes evident that the transportation of both relief supplies and evacuees will inevitably occupy limited logistics resources (i.e., road capacity). Therefore, when constructing a model for solving both FLIP and HEP, the uncertainty of road capacity should be incorporated into the model framework.

At present, the prevailing methodologies for addressing the aforementioned uncertainties fall into two categories: stochastic programming (SP) approaches and robust optimization (RO) approaches. The fundamental idea of the SP is to construct specific scenarios, with the assumption that each scenario has a probability of occurrence. Therefore, the use of this type of method is inseparable from the accurate probability distribution information of the uncertainty parameters. Sample average approximation (SAA) is a common method for dealing with SPs; however, the limited information on historical disasters makes it difficult for us to know the specific distribution information (El Tonbari et al., 2024; Zhang et al., 2025). Even if a scenario-based SP optimization model is constructed on the basis of a biased probability distribution (i.e., we estimate this distribution function based on limited sample data), the obtained solution is likely to exhibit low reliability. This phenomenon is referred to as *optimization bias* (Smith & Winkler, 2006). In light of the aforementioned modeling deficiencies, several researchers have begun to focus on the idea of using RO theory to address uncertainty. To characterize uncertain parameters, this approach constructs *uncertainty sets*. Nevertheless, RO theory aims to enhance the worst case (i.e., scenario) under uncertainty sets, which often makes optimal solutions overly conservative, and the cost remains high (Baron et al., 2011). In recent years, with the development of uncertain optimization theory, distributionally robust optimization (DRO) has become a cutting-edge tool that bridges the gap between the requirements of the SP approach for known distribution functions and the tendency of the RO approach to produce overly conservative solutions. This tool requires only partial information about the distribution, yet it is also capable of reducing the detrimental effects of distributional ambiguity. As a result, it is frequently employed in the mathematical modeling of uncertainty problems in humanitarian relief logistics management (e.g., Gao and Kleywegt (2023) and Yin et al. (2024b)).

Motivated by the disconnect between existing FILP and HEP studies and the limitations of the SP and RO methods in addressing uncertainty, this paper aims to investigate the collaborative optimization problem of FLIP and HEP considering uncertainty factors (hereafter referred to as FLI-HEP) and model it as a two-stage DRO model. Specifically, the *preparation-stage* corresponds to pre-disaster decisions considered by the decision maker, including facility location and inventory pre-positioning. The *response-stage* corresponds to post-disaster decisions considered by the decision maker, including relief supply transportation and human evacuation planning. Two types of uncertain parameters are considered in this model: (1) the number of evacuees and (2) the post-disaster road capacity. The research question we attempt to answer in this paper is as follows:

Research question. *Suppose that the number of evacuees and the post-disaster road capacity are uncertain parameters and that the decision maker (e.g., government) has only limited historical data associated with disasters. Two types of flows (i.e., relief supply flow and evacuee flow) exist simultaneously in the HRLN and occupy limited and uncertain road capacity after a disaster. How does the decision maker solve the FLI-HEP?*

Overall, this paper aims to address the gap between the practice of disaster logistics and the literature. First, it is important to note that relief supply transportation and evacuee evacuation occur simultaneously after a disaster. Therefore, both should be considered within the same modeling framework. However, the topic of human evacuation activities (or relief supply transportation activities) is frequently overlooked in the existing FLIP (or HEP) literature. Second, logistics infrastructure, such as roads, is easily destroyed during disasters. The transportation of relief supplies and evacuees may simultaneously occupy this critical and vulnerable logistics resource. However, in the FLIP and HEP literature, logistics infrastructures are usually considered to be unaffected by disasters. Finally, although the FLI-HEP can be modeled via scenario-based SO or uncertainty set-based RO, the identification of scenarios and the construction of uncertainty sets present difficulties when historical data are scarce. In such cases, overly conservative or overly optimistic solutions may have adverse consequences for disaster relief. To address these challenges, we investigate the FLI-HEP within the two-stage DRO modeling framework. In general, this paper makes three contributions.

(1) We abstract an integrated HRLN design problem called the FLI-HEP. The essential difference between our FLI-HEP and established research is the consideration of two types of flows in the HRLN and road disruption factors. This allows us to consider the interaction between the two types of flows simultaneously and reflects the concept of giving equal importance to beneficiary-centric HRLN design ideas and supply-

centric HRLN design ideas during modeling. In our FLI-HEP, two types of decisions, i.e., pre-disaster decisions and post-disaster decisions, are optimized in a two-stage model. To the best of our knowledge, this is the first paper that integrates FLIP and HEP and considers the uncertainties associated with road capacity.

(2) We formulate the FLI-HEP as a two-stage DRO model. Moreover, a customized ambiguity set is constructed to capture the uncertainty in the number of evacuees and the road capacity by utilizing historical data and type-1 Wasserstein metrics. The above method is particularly suitable for problems with limited historical data, such as our FLI-HEP, and can overcome the difficulties of scenario-based SP approaches in scenario recognition and the shortcomings of the over-conservatism produced by RO approaches. Furthermore, we show that our proposed model possesses a reformulate version that can be solved by decomposition algorithms. Therefore, we develop two versions of the decomposition algorithm based on the generic Benders-decomposition technique, i.e., single-cut and multi-cut versions, to explore the global optimal solutions to our model.

(3) We use a real-world example, the Yushu earthquake in April 2010 in Qinghai Province, China, to evaluate the performance of the proposed DRO model and decomposition techniques. Our experimental results indicate that our two-stage DRO model tends to produce more robust solutions than scenario-based models do. Additionally, several managerial insights are presented to assist decision makers in conducting humanitarian relief activities effectively.

The remainder of this paper is organized as follows. A review of previous studies on FLIP and HEP in the context of HRLN design is provided in Section 2. Section 3 describes our proposed FLI-HEP and attempts to establish the DRO model to model the FLI-HEP. In Section 4, we define the type-1 Wasserstein ambiguity set. Meanwhile, this model is reformulated to another computationally tractable two-stage model based on the properties of the type-1 Wasserstein ambiguity set. To solve the reformulated model, we design two decomposition algorithms to explore the global solution in Section 5. Section 6 presents a case study. Finally, we propose the conclusions of this paper in Section 7. Several interesting future research directions are also given in this section.

2. Literature review

Since the FLI-HEP involved in this paper is a composite problem of FLIP and HEP, this section conducts a literature review of these two types of research. The rampant disaster events in recent years have brought tremendous pressure to the existing HRLN, leading to more attention to research questions associated with disaster management. Several systematic literature reviews have been conducted based on different research perspectives, such as production operations management (Gupta et al., 2016), inventory management (Ye et al., 2020), and operations research (Besiou et al., 2018). Before conducting our literature review, we use Table 1 to organize the research methods of the important literature involved in this section. In this table, we use the decision column to represent the decisions involved by the decision maker, including the four most common decisions: location decisions, inventory level decisions, transportation decisions and evacuation decisions. Specifically, location decisions and inventory-level decisions determine where and how much to pre-position relief supplies at each facility (e.g., distribution centers and relief shelters), respectively. The transportation decision determines the quantity of relief supply to be transported between facilities and disaster areas. Finally, the evacuation decision considers where and how many evacuees should be transported from the disaster area.

2.1. Facility location and inventory pre-positioning in humanitarian logistics

In recent years, research on FLIP has been widely carried out. This research paradigm can also be called a supply-centric paradigm, which means that ensuring the effective transportation of relief supplies is the core concern of decision makers during the modeling process. For a systematic review, one can refer to Sabbaghtorkan et al. (2020). The representative literature includes Rawls and Turnquist (2010), who considered the minimization of total cost through the analysis of the pre-positioning of different types of relief supplies. The authors abstracted the problem as a two-stage SP and developed a Lagrangian L-shaped algorithm to address the model. Later, Tofighi et al. (2016) investigated a similar problem, except that the transportation time was also taken as one of the optimization objectives. To handle this multi-objective optimization problem, the approach of weighting different objectives was adopted, and a meta-heuristic algorithm called the differential evolution algorithm was developed to explore some satisfactory solutions of the model. Noham and Tzur (2018) considered several humanitarian constraints (the author called them *equitable allocation policy* and *preferred assignment policy*) in the model to ensure that the relief supplies were

Table 1
Research on the papers associated with our FLI-HEP.

Reference	Decision	Objective	Uncertainty	Model formulation	Algorithm
Rawls and Turnquist (2010)	L/I/T	Cf/Ch/Ct/Cp	D/Lc/S	SP (two-stage)	Ls
Tofighi et al. (2016)	L/I/T	Cf/Ch/Ct/Cp	D/Lc/S	SP (two-stage)	M
Noham and Tzur (2018)	L/T	Co/Crt	D	SP	M
Erbeyoğlu and Bilge (2020)	L/I/T	Cf/Ch	D	RO	B
Pouraliakbari-Mamaghani et al. (2023)	I/T	Crt	D/Lc/S	RO (two-stage)	C
Zhang et al. (2023)	L/I/T	Cf/Ch/Ct/Cp	D/Lc	DRO (two-stage)	Ls/H
Ng and Waller (2010)	Ev	Ce	D/Lc	MIP	–
Özdamar and Demir (2012)	T/Ev	Ce	None	MIP	H
Shahparvari et al. (2016)	Ev	Cf/Ce	Lc	MIP	–
Rambha et al. (2021)	Ev	Cf/Ct/Car/Ri	Lc	SP	–
Wang et al. (2021)	L/I/T/Ev	Cf/Ch/Ct/Cp	E/Tr	SP (two-stage)	B
Dalal and Üster (2021)	L/T/Ev	Cf/Ct	E	RO	B
Yin et al. (2024b)	L/T/Ev	Cf/Crc	D/Lc	RO (two-stage)	B
Yin et al. (2024a)	L/I/T/Ev	Cf/Ch/Ct/Cp/Ce	D	DRO	BC
This paper	L/I/T/Ev	Cf/Ch/Ct/Cp/Ce	D/Lc/E	DRO (two-stage)	Ls

Note:
(1) L: Location, I: Inventory level, T: Supply transportation, Ep: Human evacuation.
(2) Cf: Fixed cost of opening a facility, Ch: Relief inventory holding cost, Ct: Relief supply transportation cost, Cp: Penalty cost, Co: Coverage, Crt: Response time; Ce: Evacuation cost, Crc: Recovery cost, Ri: Risk, Car: Cost of care.
(3) D: Demand, Lc: Logistics infrastructure condition, S: Storage state, E: Evacuation rates, Tr: Travel time.
(4) RO: Robust optimization, SP: stochastic programming, MIP: Mixed-integer programming, DRO: Distributionally robust optimization.
(5) Ls: L-shaped method, M: meta-heuristic algorithm, B: Benders decomposition, C: Column-and-constraint-generation, H: heuristic algorithm, BC: branch-and-Benders-cut algorithm.

transported in a fair manner. This research paradigm is based on the supply-centric paradigm and embodies some beneficiary-centric philosophies. The authors directly used the solver to solve small-scale problems and designed a tabu-search method specifically for large-scale problems. In terms of research methodology, all of the above studies used the SP method. In recent years, RO has also been adopted by the academic community as an important theory used in solving FLIP. For example, Erbeyoğlu and Bilge (2020) implemented a similar idea as Noham and Tzur (2018), emphasizing more service adequacy and fairness in the model rather than taking the lowest cost as the decision maker's priority strategy. Pouraliakbari-Mamaghani et al. (2023) specifically considered the congestion factor in relief facilities in the model framework. They suggested that large quantities of relief supplies transported to a facility create queues and additional penalty waiting time. Therefore, the authors applied a stochastic-robust optimization approach. To achieve an exact solution of the optimization model, a column-and-constraint generation approach was developed. Very recently, with the development of DRO theory, Zhang et al. (2023) constructed a DRO model. They incorporated road condition enhancement strategies into pre-disaster decision making by introducing type-1 Wasserstein ambiguity sets, allowing decision makers to take the necessary means to perform road enhancements before a disaster occurs to reduce the risk of road damage from a disaster. Considering the uncertainty associated with the demand of relief supply and post-disaster road capacity, the authors constructed a two-stage DRO and designed both an exact algorithm and a heuristic algorithm to explore the solution of the model.

Based on the above literature, it can be seen that scholars currently consider three model frameworks—SP, RO and DRO—when modeling FLIP. Especially in recent years, DRO has gradually become a mainstream modeling approach. In terms of the factors considered, an increasing number of studies are incorporating realistic factors (e.g., queuing and supply allocation fairness) into the model framework. In particular, as understanding has deepened, the academic community has begun to take into account the beneficiary-centric research paradigm in supply-centric problems by adding corresponding constraints. However, such studies are ultimately based on a supply-centric research paradigm and have not been able to simultaneously consider HEP in the modeling framework. For example, in the study of FLIP, the location decision is limited to the distribution centers (where only the relief supplies are stored), and the location of the rescue shelters (where evacuees are evacuated) is not considered. Moreover, human evacuation activities also occupy the limited capacity of logistics facilities (e.g., road capacity). Ignoring this behavior when considering FLIP is equivalent to ideally assuming that evacuating people has no effect on the capacity of logistics facilities. This contradicts the current situation in which the transportation of evacuees and relief supplies occurs simultaneously.

2.2. Human evacuation planning in humanitarian relief networks

In contrast to the research on FLIP, the research on HEP adopts a beneficiary-centric research paradigm because the core decision of this type of problem is the evacuation of evacuees. Early on, Ng and Waller (2010) discussed the HEP based on cell transmission theory, laying the foundation for this type of research. Özdamar and Demir (2012) introduced the concept of *hierarchical clustering* and developed a clustering algorithm to cluster nodes with different evacuation demands, which is conducive to the subsequent optimization process. Considering the problem complexity, the authors directly constructed a deterministic MIP and solved it via the commercial solver CPLEX. Shahparvari et al. (2016) incorporated the uncertainty of road capacity and shelter capacity into a model framework during the evacuation process. However, in order to address this uncertainty, the authors used a method to calculate the risk level of different road segments and calculate the actual capacity of logistics facilities based on the abovementioned risk level. Thus, the investigated problem was reformulated into a deterministic problem. With the development of theory and deepening understanding in recent years, the use of scenario-based SPs has gradually become an effective tool for modeling HEPs. For example, Rambha et al. (2021) established a scenario-based SP that considered different types of patients. By constructing different scenarios, the authors modeled the different evolution processes of disaster events (i.e., storms). Under different scenarios, the capacity of logistics infrastructure (i.e., road, electricity and communications) is different. Since 2021, scholars have considered the allocation of relief supplies (i.e., the interaction between human evacuation and supply-side inventory management/supply allocation) during the evacuation process. This reflects a paradigm shift from being beneficiary-centric to being both supply-centric and beneficiary-centric. For example, Wang et al. (2021) constructed a scenario-based SP and considered the key disaster information of mobile phone location data. The authors designed a customized Dantzig–Wolfe decomposition algorithm to achieve an accurate solution of this scenario-based SP. Dalal and Üster (2021) established an RO model to optimize facility locations and relief supply quantities. The difference from Wang et al. (2021) is that the authors considered different modes of transport and developed a Benders decomposition algorithm. Very recently, following Dalal and Üster (2021), Yin et al. (2024b) established a two-stage RO model that considers the capacity uncertainty of two types of logistics facilities, namely, relief facilities and roads, and a two-stage decomposition algorithm was designed. In addition, the authors also considered a variety of mitigation strategies (e.g., facility reopening and sharing of relief supplies) to make this model more realistic.

From the perspective of research methods, we can conclude that early research focused on building deterministic MIPs that can be solved by commercial solvers. In recent years, RO and SP have remained the mainstream methods for addressing HEP. From the perspective of practical factors considered, researchers have comprehensively considered various possible uncertainties and gradually incorporated several possible factors (e.g., different modes of transportation and resource sharing) into the model framework. However, such studies are still insufficient in terms of the interaction between factors involved in FLIP. Therefore, the current lack of research on the collaborative optimization of FLIP and HEP motivates us to conduct specific research on this topic to increase the adaptability of the optimization technique and theory to the complex needs of reality. To the best of our knowledge, although FLI-HEP has the potential to establish reliable HRLNs, this research question has not yet been investigated in the literature. The research most similar to our FLI-HEP is a composite problem of FLIP and HEP raised by Yin et al. (2024a). The authors developed a one-stage model with several individual chance constraints to solve a relaxed FLIP-HEP, and their modeling ideas still have the following shortcomings. First, the authors assumed that the capacity of each road segment is infinite and is not affected by disasters. Based on this assumption, the authors did not optimize the specific transportation plan for relief supplies and evacuees but directly assigned them according to the principle of shortest route (or shortest cost). This assumption is overly idealistic compared with the actual situation. Meanwhile, it also causes the problem addressed by the authors to be not completely equivalent to the standard FLIP-HEP. Second, the authors assumed that the number of injured people who need to be evacuated in each time period is known and did not consider providing relief supplies to the uninjured; instead, they assumed that the per capita relief supply demand for the injured is a random variable. This assumption is also inconsistent with the actual situation. Typically, relief supplies should be provided to people in disaster areas regardless of whether they are injured or not. The per capita demand for most relief supplies (e.g., tents, food, drinking water) is relatively stable. Finally, the authors constructed an ambiguity set based on moment information, which easily leads to overly conservative solutions. Meanwhile, it lacks some attractive statistical properties in comparison with the Wasserstein ambiguity set (Ho-Nguyen et al., 2022). To address the above shortcomings, our proposed FLI-HEP emphasizes the following points. First,

our proposed FLIP-HEP acknowledges that both types of flows compete for limited and uncertain logistics resource (i.e., roads) capacity. Thus, the optimization of transportation schemes for relief supplies and evacuees is considered. Second, we consider the uncertainty of the number of evacuees and do not limit the relief supply to only those who need to be evacuated, thus making the model more consistent with actual operational situations. Third, we develop a model based on the Wasserstein ambiguity set so that we can use its mathematical properties to easily complete the model transformation.

3. Problem description and model formulation

As mentioned earlier, we establish a two-stage DRO model that simultaneously incorporates the uncertainty of the number of evacuees caused by the disaster and the post-disaster road capacity to address the FLI-HEP. The abovementioned two stages are related to the decisions made by decision makers in the pre-disaster and post-disaster stages, respectively. To this end, we first present the problem description of the FLI-HEP in Section 3.1. In Section 3.2, we develop a basic two-stage SP model to lay the foundation for subsequent DRO model transformation.

3.1. Problem description

The FLI-HEP is described in Fig. 1. Specifically, in the preparation-stage (see the left part of Fig. 1), decision makers prepare by opening one or more facilities (e.g., distribution centers) to store relief resources and one or more facilities (e.g., rescue shelters) to simultaneously store relief resources and shelter evacuees. The location, size of each open facility, and quantity of relief supplies to be pre-positioned in each open facility should be determined in advance by decision makers. Because large donations are usually received only after a disaster occurs (Stauffer & Kumar, 2021), decision makers usually control costs in their pre-disaster preparations. Therefore, we assume that the decision maker has an upper limit on the budget and (s)he aims at minimizing the total cost of pre- and post-disaster relief operations, including (1) the fixed costs associated with facility openings, (2) the inventory holding costs of relief supplies, (3) the relief supplies (evacuees) transportation costs, (4) the inventory shortage penalty costs, and (5) penalty costs for failure to evacuate evacuees. After the random variables (i.e., the number of evacuees and road capacity) are realized, the decision maker proceeds to the response-stage of decision-making (see the right part of Fig. 1), which considers the transportation scheme of relief supplies to meet the demands of the victims, as well as the evacuation plan for evacuees.

Considering that there are two types of flows in the HRLN, we establish a multi-commodity network enabling the evacuation of evacuees and the transportation of relief supplies (e.g., food and clothing). The corresponding HRLN is abstracted by graph $G = (N, A)$, where $N = N_P \cup N_D \cup N_R \cup N_O$. Here, N_P, N_D, N_R and N_O denote the sets of disaster areas, candidate locations of distribution centers, candidate locations of rescue shelters and dummy nodes, respectively. Set A represents the set of roads (i.e., links) in the HRLN. Each node $i \in N_P$ denotes a disaster area with a total population of p_i, and it is associated with an exogenous random variable $\widetilde{\delta}_i$, which denotes the proportion of evacuees to the total population in area $i \in N_P$ and is realized in interval $[\underline{\delta}_i, \overline{\delta}_i]$. In this way, we can use term $p_i\widetilde{\delta}_i$ to represent the number of evacuees (note that it is uncertain) who need to be evacuated in area $i \in N_P$. Correspondingly, the stay-back population in area $i \in N_P$ can be expressed as $p_i\left(1-\widetilde{\delta}_i\right)$. Each node $i \in N_D$ is a candidate location of distribution centers with a lower limit $\underline{Q}^{DS}$ (i.e., minimum relief supply storage required to open a center) and an upper limit $\overline{Q}_i^{DS}$ for the storage of relief supplies, where decision makers can place some relief supplies in advance. Each node $i \in N_R$ is a candidate location of rescue shelters with a maximum evacuee capacity SH_i, a lower limit $\underline{Q}^{RS}$ (i.e., minimum relief supply storage required to open a rescue shelter), and an upper limit $\overline{Q}_i^{RS}$ for the storage of relief supplies. Considering that a disaster area can also store relief supplies, we assume that $N_D \supseteq N_P$. Meanwhile, considering the possibility of secondary disasters in the disaster area, we assume that $N_P \cap N_R = \varnothing$. Since rescue shelters can store relief supplies, we also assume that $N_D \cap N_R = \varnothing$. This assumption can be relaxed by introducing an additional dummy node for the location that is suitable for establishing both a distribution center and a rescue shelter. Let x_i represent a 0−1 decision variable that takes a value of 1 if the candidate facility at point $i \in N_D \cup N_R$ is open with a fixed cost F_i^1 and 0 otherwise; h_i denotes the decision variable of the quantity of relief supply pre-positioned at facility $i \in N_D \cup N_R$ with an inventory holding cost per unit quantity F_i^2. The dummy node $i \in N_O$ can be added to a road to divide it into different segments. Thus, we can characterize the different capacities of the road at different segments.

Before a disaster occurs, the initial capacity of link (i, j) is represented as CAP_{ij}, which represents the maximum flow that vehicles can pass through it in a certain period of time (e.g., one day; see the definition in Zhang et al. (2023)). After a disaster, the capabilities of some links may be impaired. Following prior studies (e.g., Ni et al. (2018), Zhang et al. (2023) and Che et al. (2024)), we measure this loss via a random

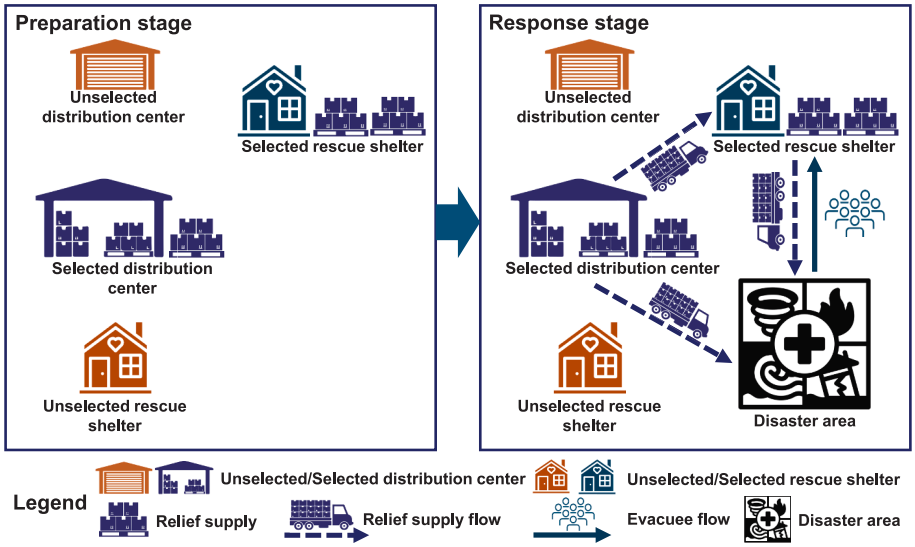

Fig. 1. Illustration of the FLI-HEP.

variable $\widetilde{\xi}_{ij}$, which is realized in interval $[0,1]$. Specifically, when $\widetilde{\xi}_{ij} = 0$, link $(i,j) \in A$ is completely damaged. In contrast, $\widetilde{\xi}_{ij} = 1$ means that the capacity of this link is not affected by the disaster. After the disaster, the actual capacity of link (i,j) can be expressed as $CAP_{ij}\widetilde{\xi}_{ij}$. For convenience, the commonly used notations in this paper are listed below.

Sets	
N	Set of nodes in graph G, whose elements are denoted as i or j
N_P	Set of disaster areas
N_D	Set of (candidate location of) distribution centers
N_R	Set of (candidate location of) rescue shelters
N_O	Set of dummy nodes
A	Set of links in graph G, whose elements are denoted as (i,j)
K	Set of types of flows, whose elements are denoted as k
$\mathbb{F}_W$	Type-1 Wasserstein ambiguity set
$\mathbb{R}_+$	Set of non-negative real numbers
$[N]$	A set containing the integers from 1 to N, i.e., $[N] := \{1,2,\cdots,N\}$
Parameters	
$\mathbb{P}$	A probability distribution function of random vector
F_i^1	The fixed cost for opening one distribution center (or rescue shelter) at node $i \in N_D \cup N_R$
F_i^2	The unit inventory handing cost at node $i \in N_D \cup N_R$
B	The budget ceiling for the decision maker
$\underline{Q}^{RS}$, $\underline{Q}^{DS}$	The minimum relief supply storage at a distribution center or rescue shelter
$\overline{Q}_i^{RS}$, $\overline{Q}_i^{DS}$	The maximum relief supply storage at a distribution center or rescue shelter $i \in N_D \cup N_R$
C_{ijk}^1	The unit transportation cost of type k flow transported by link $(i,j) \in A$
C_i^2	The unit penalty cost of relief supply shortage on node $i \in N_P \cup N_R$
C_i^3	The unit penalty cost for failure to evacuate population on node $i \in N_P$
CAP_{ij}	The initial capacity of link $(i,j) \in A$
p_i	The total population on disaster area $i \in N_P$
d	The demand for relief supply for a person
SH_i	The maximum evacuee capacity of rescue shelter $i \in N_R$
Random variables	
$\widetilde{\delta}_i$	Random variable associated with proportion of evacuees to the total population at node $i \in N_P$, where $\widetilde{\boldsymbol{\delta}} = \left(\widetilde{\delta}_i\right)$
$\widetilde{\xi}_{ij}$	Random variable associated with capacity of link $(i,j) \in A$ after disaster, where $\widetilde{\boldsymbol{\xi}} = \left(\widetilde{\xi}_{ij}\right)$
$\widetilde{\boldsymbol{\zeta}}$	Random vector, where $\widetilde{\boldsymbol{\zeta}} = \left(\widetilde{\boldsymbol{\delta}}, \widetilde{\boldsymbol{\xi}}\right)^{\mathrm{T}}$
Preparation-stage decision variables	
x_i	A binary variable, which represents whether facility at node (i.e., candidate location) $i \in N_D \cup N_R$ is opened
h_i	A continuous variable, which represents the quantity of pre-position relief supply on facility located at node (i.e., candidate location) $i \in N_D \cup N_R$
Response-stage decision variables	
y_{ij}^k	A continuous variable, which represents the flow volume of k^{th} class of flows on link $(i,j) \in A$
s_i	A continuous variable, which represents the shortage quantity of supply at node $i \in N_P \cup N_R$
r_i	A continuous variable, which represents the number of evacuees that has not evacuated from node $i \in N_P$

3.2. Basic two-stage stochastic programming model

Based on the above discussion, we propose a basic two-stage SP model in this subsection, which is the basis for constructing the DRO model. Then, in Section 4, we present the two-stage DRO model. The preparation-stage SP model of the FLI-HEP can be developed as follows.

Preparation-stage SP model:

$$\min_{(\boldsymbol{x},\boldsymbol{h})} \left\{ \sum_{i \in N_D \cup N_R} \left(F_i^1 x_i + F_i^2 h_i\right) + \mathbb{E}_{\mathbb{P}}[g(\boldsymbol{x},\boldsymbol{h},\widetilde{\boldsymbol{\zeta}})] \right\} \tag{1a}$$

$$s.t. \sum_{i \in N_D \cup N_R} \left(F_i^1 x_i + F_i^2 h_i\right) \leqslant B \tag{1b}$$

$$\underline{Q}^{RS} x_i \leqslant h_i \leqslant \overline{Q}_i^{RS} x_i \forall i \in N_R \tag{1c}$$

$$\underline{Q}^{DS} x_i \leqslant h_i \leqslant \overline{Q}_i^{DS} x_i \forall i \in N_D \tag{1d}$$

$$\boldsymbol{x} \in \{0,1\}^{|N_D \cup N_R|},\ \boldsymbol{h} \in \mathbb{R}_+^{|N_D \cup N_R|}, \tag{1e}$$

where vector $\widetilde{\boldsymbol{\zeta}} = \left(\widetilde{\boldsymbol{\delta}}, \widetilde{\boldsymbol{\xi}}\right)^{\mathrm{T}} \in \Xi \subseteq \mathbb{R}_+^{|N_P|} \times \mathbb{R}_+^{|A|}$; B denotes the upper limit on the budget; $\mathbb{P}$ represents the probability distribution function of random vector $\widetilde{\boldsymbol{\zeta}}$; $\boldsymbol{x} = (x_i)$; and $\boldsymbol{h} = (h_i)$.

The function (1a) requires minimizing the total cost (i.e., the sum of the facility opening cost $F_i^1 x_i$, relief supply inventory handling cost $F_i^2 h_i$, and expected response-stage cost $\mathbb{E}_{\mathbb{P}}[g(\boldsymbol{x},\boldsymbol{h},\widetilde{\boldsymbol{\zeta}})]$ associated with random vector $\widetilde{\boldsymbol{\zeta}} = \left(\widetilde{\boldsymbol{\delta}}, \widetilde{\boldsymbol{\xi}}\right)^{\mathrm{T}}$). Note that the bounded supporting space $\Xi = \left\{ \widetilde{\boldsymbol{\zeta}} = \left(\widetilde{\delta}_i, \widetilde{\xi}_{ij}\right) \in \mathbb{R}_+^{|N_P|} \times \mathbb{R}_+^{|A|} \,\middle|\, \widetilde{\delta}_i \in [\underline{\delta}_i, \overline{\delta}_i], \widetilde{\xi}_{ij} \in [0,1], \forall i \in N_P, \forall (i,j) \in A \right\}$. Constraint (1b) requires that the preparation-stage cost does not exceed the budget limit. Constraints (1c) and (1d) require that the quantity of the relief supply pre-positioned at node i is greater than or equal to the minimum quantity to open a facility and less than or equal to the capacity limitation if the decision maker opens a facility at node i. Finally, we use constraint (1e) to restrict the domain of decision vector $(\boldsymbol{x},\boldsymbol{h})^{\mathrm{T}}$. For simplicity in the subsequent description, the feasible region of this preparation-stage model is represented as set $\boldsymbol{dom}_1 = \left\{ (\boldsymbol{x},\boldsymbol{h})^{\mathrm{T}} \,\middle|\, \text{Constraints (1b)} - \text{(1e)} \right\}$.

Given decision vector $(\boldsymbol{x},\boldsymbol{h})^{\mathrm{T}}$ and realization $\widetilde{\boldsymbol{\zeta}}$, we further establish the response-stage model. To differentiate between two types of flows within the HRLN, we use K to denote the set of types of flows, whose elements are denoted as k. Specifically, we use $k = 1$ to denote the evacuee flow and $k = 2$ to represent the relief supply flow. For each link, we use variable y_{ij}^k to represent the flow volume of type k flow on this link, where $\boldsymbol{y} = \left(y_{ij}^k\right)$. Usually, since different types of flows may have different "consumptions" of road capacity, we use the coefficient Fac_k to relate the k^{th} type of flow to the link capacity. This approach is also used in Rawls and Turnquist (2010), Noyan (2012), Xin et al. (2025), and Che et al. (2024). The transportation cost of a unit of relief supply (or an evacuee) on link $(i,j) \in A$ is denoted by C_{ijk}^1. Let d be the quantity of relief supply demanded by one person. We set the relief supply shortage amount at node $i \in N_P \cup N_R$ to s_i, where $\boldsymbol{s} = (s_i)$, and the associated unit penalty cost is C_i^2. Similarly, we let r_i denote the number of evacuees who have not evacuated from node $i \in N_P$, where $\boldsymbol{r} = (r_i)$, and the penalty cost of one person not being evacuated is C_i^3. Based on the abovementioned notation, the response-stage model is proposed to optimize $(\boldsymbol{y},\boldsymbol{s},\boldsymbol{r})^{\mathrm{T}}$.

Response-stage SP model:

$$g(\boldsymbol{x},\boldsymbol{h},\widetilde{\boldsymbol{\zeta}}) = \min_{(\boldsymbol{y},\boldsymbol{s},\boldsymbol{r})} \left\{ \sum_{k \in K} \sum_{(i,j) \in A} C_{ijk}^1 y_{ij}^k + \sum_{i \in N_P \cup N_R} C_i^2 s_i + \sum_{i \in N_P} C_i^3 r_i \right\} \tag{2a}$$

$$s.t. \sum_{k \in K} Fac_k y_{ij}^k \leqslant CAP_{ij}\widetilde{\xi}_{ij} \quad \forall (i,j) \in A \tag{2b}$$

$$\sum_{j:(j,i) \in A, k=1} y_{ji}^k - \sum_{j:(i,j) \in A, k=1} y_{ij}^k \geqslant \begin{cases} p_i\left(1 - \widetilde{\delta}_i\right) d - s_i & \text{if } i \in N_P \\ -h_i & \text{if } i \in N_D \\ SH_i d - h_i - s_i & \text{if } i \in N_R \\ 0 & \text{if } i \in N_O \end{cases} \tag{2c}$$

$$\sum_{j:(j,i) \in A, k=2} y_{ji}^k - \sum_{j:(i,j) \in A, k=2} y_{ij}^k \leqslant \begin{cases} -p_i\widetilde{\delta}_i + r_i & \text{if } i \in N_P \\ 0 & \text{if } i \in N_D \cup N_O \\ SH_i & \text{if } i \in N_R \end{cases} \tag{2d}$$

$$\boldsymbol{y} \in \mathbb{R}_+^{|A| \times |K|},\ \boldsymbol{s} \in \mathbb{R}_+^{|N_P \cup N_R|},\ \boldsymbol{r} \in \mathbb{R}_+^{|N_P|}. \tag{2e}$$

The objective function (2a) minimizes the total cost associated with the response-stage decisions, including the transportation costs of the relief supply and the evacuation costs of evacuees $C^1_{ijk}y^k_{ij}$, as well as the penalty costs due to the shortage of the relief supply $C^2_i s_i$ and the failure to evacuate evacuees $C^3_i r_i$. Although the model does not contain the first-stage decision vector $\boldsymbol{x}$, we still use $g(\boldsymbol{x}, \boldsymbol{h}, \widetilde{\boldsymbol{\xi}})$ to describe the objective function of this stage to maintain completeness. In this paper, we consider only two types of flows that jointly occupy a limited road capacity, and Constraint (2b) is the capacity constraint. Constraints (2c) and (2d) are the network flow balance constraints for relief supply flow and for evacuation flow, respectively. Finally, we use constraint (2e) to restrict the domain of decision vector $(\boldsymbol{y}, \boldsymbol{s}, \boldsymbol{r})^{\mathrm{T}}$. For simplicity, set $\boldsymbol{dom}_2 = \{(\boldsymbol{y}, \boldsymbol{s}, \boldsymbol{r})^{\mathrm{T}} \,|\, \text{Constraints (2b)} - \text{(2e)}\}$ is used to indicate the feasible region of the above response-stage model.

In daily disaster relief practice, since the decisions involved in the first-stage model are made before the random variables are realized, the true probability distribution of the random vector cannot be accurately known. This poses a challenge in solving the model. Nevertheless, the distribution function $\mathbb{P}$ can often be partially observed through a finite set of independent samples (e.g., the historical realizations of the random vector). Sometimes, scholars also directly assume that the distribution function $\mathbb{P}$ is known and generate a finite set of independent samples based on $\mathbb{P}$. We denote N known independent samples of vector $\widetilde{\boldsymbol{\xi}}$ as $\widehat{\boldsymbol{\xi}}^1, \widehat{\boldsymbol{\xi}}^2, \ldots, \widehat{\boldsymbol{\xi}}^N$. With these samples, the SAA approach can be used to approximate $\mathbb{P}$. At this point, the first-stage SP model can be rewritten as follows. Here, we assume that each sample unit has an equal probability of occurring.

$$J_{\mathrm{SAA}} = \min_{(\boldsymbol{x},\boldsymbol{h})\in \boldsymbol{dom}_1} \left\{ \sum_{i\in N_D\cup N_R} \left(F^1_i x_i + F^2_i h_i\right) + \frac{1}{N}\sum_{n\in[N]} g(\boldsymbol{x}, \boldsymbol{h}, \widehat{\boldsymbol{\xi}}^n) \right\}.$$

Typically, solutions obtained via the abovementioned SAA method tend to lead to poor out-of-sample performance, especially when historical information is limited (Bertsimas & Thiele, 2006). In addition, overfitting is likely to occur when this method is used, especially when the dimension of the random vector is high and the prior samples are non-stationary (Hao et al., 2020). Considering the above situation, we further transform the original two-stage SP model into a two-stage DRO model in Section 4.

4. Model reformulation

DRO theory posits that although the true distribution $\mathbb{P}$ of a random variable is unknown, it lies within an *ambiguity set*, which effectively addresses the decision maker's lack of knowledge about the distribution information. We denote the abovementioned ambiguity set as $\mathbb{F}$ and establish it using the type-1 Wasserstein metric and a set of historical data (samples). For simplicity, the two-stage model proposed in Section 3 is equivalently written as the following model.

DRO:

$$\min_{(\boldsymbol{x},\boldsymbol{h})\in \boldsymbol{dom}_1} \left\{ \sum_{i\in N_D\cup N_R} \left(F^1_i x_i + F^2_i h_i\right) + \sup_{\mathbb{P}\in\mathbb{F}} \mathbb{E}_{\mathbb{P}}[g(\boldsymbol{x}, \boldsymbol{h}, \widetilde{\boldsymbol{\xi}})] \right\} \tag{3}$$

where $g(\boldsymbol{x}, \boldsymbol{h}, \widetilde{\boldsymbol{\xi}}) = \min_{(\boldsymbol{y},\boldsymbol{s},\boldsymbol{r})\in \boldsymbol{dom}_2} \sum_{k\in K}\sum_{(i,j)\in A} C^1_{ijk} y^k_{ij} + \sum_{i\in N_P\cup N_R} C^2_i s_i + \sum_{i\in N_P} C^3_i r_i.$

It can be observed that a key element in the above model is $\mathbb{F}$. A well-designed ambiguity set $\mathbb{F}$ can effectively enhance the computational tractability (i.e., we need the real-scale problem to be solvable in a reasonable time), as well as the out-of-sample performance. In contrast, inappropriate ambiguity set construction may cause over-conservatism solutions. To this end, the type-1 Wasserstein ambiguity metric is applied to design the ambiguity set. The subsequent subsections are organized as follows. In Section 4.1, we first introduce the basic concepts of this ambiguity set. Based on the type-1 Wasserstein ambiguity set, Section 4.2 reformulates our two-stage model into an equivalent and computationally tractable formulation, which lays the foundation for constructing an exact algorithm for solving this two-stage DRO model.

4.1. Type-1 Wasserstein ambiguity set

Although the distribution function of the random vector $\widetilde{\boldsymbol{\xi}}$ is unknown, we assume that it is in an ambiguity set $\mathbb{F}$ according to DRO theory. With the development of information technology, historical data of random parameters involved in uncertainty problems are becoming easier to obtain. To obtain the probability distribution of $\widetilde{\boldsymbol{\xi}}$, it is reasonable to approximate the true probability distribution through the *empirical distribution* $\widehat{\mathbb{P}}_N$, which corresponds to historical data (samples). We assume that N known independent samples of vector $\widetilde{\boldsymbol{\xi}}$ be represented by $\widehat{\boldsymbol{\xi}}^1, \widehat{\boldsymbol{\xi}}^2, \ldots, \widehat{\boldsymbol{\xi}}^N$. The abovementioned empirical distribution $\widehat{\mathbb{P}}_N$ can be further estimated as $\widehat{\mathbb{P}}_N = 1/N\sum_{n\in[N]}\delta_{\widehat{\boldsymbol{\xi}}^n}$, where $\delta_{\widehat{\boldsymbol{\xi}}^n}$ represents the *Dirac distribution* (a function representing the density distribution) concentrating unit mass at $\widehat{\boldsymbol{\xi}}^n$. This definition means that distribution $\widehat{\mathbb{P}}_N$ is a discrete uniform distribution associated with N pieces of historical data (N samples), and it regards each piece of historical data (sample) as a support point with a probability of $1/N$, i.e., $\widehat{\mathbb{P}}_N\{\widetilde{\boldsymbol{\xi}}^\dagger = \widehat{\boldsymbol{\xi}}^n\} = 1/N$, where $\widetilde{\boldsymbol{\xi}}^\dagger$ is the *empirical random vector* associated with random vector $\widetilde{\boldsymbol{\xi}}$. Based on the above concepts, we use Definition 1 to describe the type-1 Wasserstein ambiguity set.

Definition 1. Let $\mathscr{P}_0(\Xi)$ be the set of probability distributions of a random vector supported on Ξ. Given N samples of this random vector, the corresponding empirical distribution $\widehat{\mathbb{P}}_N$, and the type-1 Wasserstein metric $dis_W(\cdot,\cdot) : \mathscr{P}_0(\Xi)\times\mathscr{P}_0(\Xi)\mapsto[0,+\infty)$, the type-1 Wasserstein ambiguity set $\mathbb{F}_W$ can be defined as

$$\mathbb{F}_W = \{\mathbb{P}\in\mathscr{P}_0(\Xi) : dis_W(\mathbb{P}, \widehat{\mathbb{P}}_N)\leqslant\theta\} \tag{4}$$

where θ is a pre-determined non-negative parameter.

It should be noted that the abovementioned set $\mathbb{F}_W$ includes all probability distributions in the ball with the type-1 Wasserstein metric as the measure, $\widehat{\mathbb{P}}_N$ as the ball center and $\theta\in\mathbb{R}_+$ as the radius. In addition, the type-1 Wasserstein metric $dis_W(\mathbb{P}, \widehat{\mathbb{P}}_N)$ in (4) can be calculated by solving the model presented below.

$$dis_W(\mathbb{P}, \widehat{\mathbb{P}}_N) = \inf \mathbb{E}_{\overline{\mathbb{P}}}[\|\widetilde{\boldsymbol{\xi}} - \widetilde{\boldsymbol{\xi}}^\dagger\|]$$

$$s.t.\ (\widetilde{\boldsymbol{\xi}}, \widetilde{\boldsymbol{\xi}}^\dagger) \sim \overline{\mathbb{P}}$$

$$\widetilde{\boldsymbol{\xi}} \sim \mathbb{P}$$

$$\widetilde{\boldsymbol{\xi}}^\dagger \sim \widehat{\mathbb{P}}_N$$

$$\overline{\mathbb{P}}\{(\widetilde{\boldsymbol{\xi}}, \widetilde{\boldsymbol{\xi}}^\dagger) \in \Xi\times\Xi\} = 1$$

where $\overline{\mathbb{P}}$ is a joint distribution of random vector $\widetilde{\boldsymbol{\xi}}$ and empirical random vector $\widetilde{\boldsymbol{\xi}}^\dagger$; norm $\|\cdot\|$ is defined through $\|\zeta\| = \max\{w_+\cdot\zeta, -w_-\cdot\zeta\}$, where w_+ and w_- are two positive parameters. When we set $w_+ = w_- = 1$, $\|\cdot\|$ represents the 1-norm.

It should be noted that in comparison with other ambiguity sets designed in the literature (e.g., the moment-based set established in Liu et al. (2019)), the set $\mathbb{F}_W$ we consider is more flexible because it contains a radius parameter $\theta\in\mathbb{R}_+$ to control the conservatism of the model. Decision makers with different risk preferences can easily adjust the value of parameter $\theta\in\mathbb{R}_+$ to obtain risk-averse (a larger $\theta\in\mathbb{R}_+$) and risk-neutral (a smaller $\theta\in\mathbb{R}_+$) solutions. In fact, by adjusting θ or adding

more risk measuring indicators, decision makers' preferences for risk may be taken into account. In addition, our model, which is based on the type-1 Wasserstein ambiguity set, covers the SP model with discrete distributions as a special case. Specifically, when we set θ directly to 0, our model reduces to a two-stage SP model.

4.2. Reformulation of the two-stage model

Based on Definition 1, we can rewrite model (4) as the following model (5):

DRO-type 1-W:

$$\min_{(\boldsymbol{x},\boldsymbol{h})\in \boldsymbol{dom}_1}\left\{\sum_{i\in N_D\cup N_R}\left(F_i^1x_i+F_i^2h_i\right)+\sup_{\mathbb{P}\in\mathbb{F}_W}\mathbb{E}_{\mathbb{P}}[g(\boldsymbol{x},\boldsymbol{h},\widetilde{\boldsymbol{\zeta}})]\right\} \tag{5}$$

where $g(\boldsymbol{x},\boldsymbol{h},\widetilde{\boldsymbol{\zeta}})=\min_{(\boldsymbol{y},\boldsymbol{s},\boldsymbol{r})\in \boldsymbol{dom}_2}\sum_{k\in K}\sum_{(i,j)\in A}C_{ijk}^1y_{ij}^k+\sum_{i\in N_P\cup N_R}C_i^2s_i+\sum_{i\in N_P}C_i^3r_i$.

Note that the only difference between models (5) and (4) is that $\mathbb{F}$ is replaced by $\mathbb{F}_W$. By examining the model, we find that model (5) is an infinite-dimensional optimization problem. This is because it optimizes the worst-case expectation, which involves an infinite number of dimensions. To make our proposed model tractable, we apply a model reformulation technique proposed by El Tonbari et al. (2024) to address the worst-case expectation term in model (5). This reformulating process is introduced in Proposition 1.

Proposition 1. (**Theorem 1** of El Tonbari et al. (2024)). By introducing an auxiliary variable $\lambda\geqslant 0$, model (5) can be reformulated as a master problem (MP) and several subproblems (SUPs). The MP is written as:

MP:

$$\min_{\substack{(\boldsymbol{x},\boldsymbol{h})\in \boldsymbol{dom}_1,\\ \lambda\geqslant 0,\boldsymbol{\rho}}}\left\{\sum_{i\in N_D\cup N_R}\left(F_i^1x_i+F_i^2h_i\right)+\theta\lambda+\frac{1}{N}\sum_{n\in[N]}\rho_n\right\} \tag{6a}$$

$$s.t.\ \rho_n\geqslant\Theta_n(\boldsymbol{x},\boldsymbol{h},\lambda)\ \ \forall n\in[N] \tag{6b}$$

where the SUP associated with the n^{th} sample $\Theta_n(\boldsymbol{x},\boldsymbol{h},\lambda)$ can be defined as follows:

SUP(n):

$$\Theta_n(\boldsymbol{x},\boldsymbol{h},\lambda)=\max_{\widetilde{\zeta}\in\Xi}\{g(\boldsymbol{x},\boldsymbol{h},\widetilde{\zeta})-\lambda\mathrm{dis}(\widetilde{\zeta},\widehat{\zeta}^n)\} \tag{7}$$

where $\mathrm{dis}(\widetilde{\zeta},\widehat{\zeta}^n)$ denotes the reference distance function and $\mathrm{dis}(\widetilde{\zeta},\widehat{\zeta}^n)=\|\widetilde{\zeta}-\widehat{\zeta}^n\|$.

Remark 1. After the decomposition of the model in the above reformulation process, the two-stage DRO finally becomes a semi-infinite optimization model. The above decomposition is relatively straightforward in terms of technical implementation and does not necessitate any necessary conditions. Nevertheless, to ensure that these SUPs are feasible, model (5) requires *complete recourse* (Zhang et al., 2023). This implies that for all $(\boldsymbol{x},\boldsymbol{h})\in\boldsymbol{dom}_1$, $g(\boldsymbol{x},\boldsymbol{h},\widetilde{\zeta})$ should be feasible. It can be verified that our response-stage model meets this condition because for all decisions $(\boldsymbol{x},\boldsymbol{h})\in\boldsymbol{dom}_1$ and $\widetilde{\zeta}\in\Xi$, the response-stage model can always find a feasible solution.

However, SUP (7) still makes this model computationally intractable because of the max−min term resulting from the minimum operator and the semi-infinite nature of the model. Therefore, we formulate the dual problem of $g(\boldsymbol{x},\boldsymbol{h},\widetilde{\zeta})$ in order to eliminate the inner minimum operator in $g(\boldsymbol{x},\boldsymbol{h},\widetilde{\zeta})$, and the dual SUP $g_d(\boldsymbol{x},\boldsymbol{h},\widetilde{\zeta})$ can be expressed as:

Dual response-stage model:

$$g_d(\boldsymbol{x},\boldsymbol{h},\widetilde{\zeta})=\max_{(\boldsymbol{\varphi},\boldsymbol{\pi},\boldsymbol{\omega})}\left\{\begin{array}{c}\sum_{i\in N_P}p_i\left(1-\widetilde{\delta}_i\right)d\pi_i-\sum_{i\in N_D}h_i\pi_i+\sum_{i\in N_R}(SH_id-h_i)\pi_i\\ +\sum_{i\in N_P}p_i\widetilde{\delta}_i\omega_i-\sum_{i\in N_R}SH_i\omega_i-\sum_{(ij)\in A}\varphi_{ij}CAP_{ij}\widetilde{\xi}_{ij}\end{array}\right\} \tag{8a}$$

$$s.t.\ \pi_i-\pi_j-Fac_1\varphi_{ij}\leqslant C_{ij1}^1\ \ \forall(i,j)\in A \tag{8b}$$

$$\omega_j-\omega_i-Fac_2\varphi_{ij}\leqslant C_{ij2}^1\ \ \forall(i,j)\in A \tag{8c}$$

$$\pi_i\leqslant C_i^2\ \ \forall i\in N_P\cup N_R \tag{8d}$$

$$\omega_i\leqslant C_i^3\ \ \forall i\in N_P \tag{8e}$$

$$\varphi_{ij}\geqslant 0\ \ \forall(i,j)\in A\ \ \forall(i,j)\in A \tag{8f}$$

$$\pi_i\geqslant 0\ \ \forall i\in N_P\cup N_R \tag{8g}$$

$$\omega_i\geqslant 0\ \ \forall i\in N_P \tag{8h}$$

where $\boldsymbol{\pi}=(\pi_i)$; $\boldsymbol{\omega}=(\omega_i)$; and $\boldsymbol{\varphi}=(\varphi_{ij})$ are dual vectors.

For simplicity in the subsequent description, we denote the feasible region of this dual problem as $\boldsymbol{dom}_d=\left\{(\boldsymbol{\varphi},\boldsymbol{\pi},\boldsymbol{\omega})^{\mathrm{T}}\,\middle|\,\text{Constraints (8b)}-\text{(8h)}\right\}$, and $\boldsymbol{dom}_d$ is independent of vector $(\boldsymbol{x},\boldsymbol{h},\widetilde{\zeta})$. The existence of this feature makes $g_d(\boldsymbol{x},\boldsymbol{h},\widetilde{\zeta})$ feasible for any decision vector $(\boldsymbol{x},\boldsymbol{h})$. Therefore, strong duality exists between $g(\boldsymbol{x},\boldsymbol{h},\widetilde{\zeta})$ and $g_d(\boldsymbol{x},\boldsymbol{h},\widetilde{\zeta})$. At this time, we can derive the reformulation of **SUP(n)** as:

R-SUP(n):

$$\begin{aligned}\Theta_n(\boldsymbol{x},\boldsymbol{h},\lambda)&=\max_{\widetilde{\zeta}\in\Xi}\{g_d(\boldsymbol{x},\boldsymbol{h},\widetilde{\zeta})-\lambda\mathrm{dis}(\widetilde{\zeta},\widehat{\zeta}^n)\}\\&=\max_{\substack{(\boldsymbol{\varphi},\boldsymbol{\pi},\boldsymbol{\omega})\in\boldsymbol{dom}_d,\\ \widetilde{\zeta}=(\widetilde{\delta},\widetilde{\xi})^{\mathrm{T}}\in\Xi}}\left\{\begin{array}{c}-\sum_{(ij)\in A}CAP_{ij}\widetilde{\xi}_{ij}\varphi_{ij}+\sum_{i\in N_P}p_id\pi_i-\sum_{i\in N_P}p_id\widetilde{\delta}_i\pi_i-\sum_{i\in N_D}h_i\pi_i\\ +\sum_{i\in N_R}(SH_id-h_i)\pi_i+\sum_{i\in N_P}p_i\widetilde{\delta}_i\omega_i-\sum_{i\in N_R}SH_i\omega_i\\ -\lambda\mathrm{dis}\left(\left(\widetilde{\xi}_{ij},\widetilde{\delta}_i\right),\left(\widehat{\xi}_{ij}^n,\widehat{\delta}_i^n\right)\right)\end{array}\right\}\end{aligned} \tag{9}$$

where $\mathrm{dis}\left(\left(\widetilde{\xi}_{ij},\widetilde{\delta}_i\right),\left(\widehat{\xi}_{ij}^n,\widehat{\delta}_i^n\right)\right)=\left\|\left(\widetilde{\xi}_{ij},\widetilde{\delta}_i\right)-\left(\widehat{\xi}_{ij}^n,\widehat{\delta}_i^n\right)\right\|$ denotes the reference distance function.

However, the bilinear terms in (9), that is, $\widetilde{\xi}_{ij}\varphi_{ij}$, $\widetilde{\delta}_i\pi_i$ and $\widetilde{\delta}_i\omega_i$, still make this SUB difficult to solve. This motivates us to further introduce Theorem 1 to achieve a more tractable reformulation by introducing several binary auxiliary variables.

Theorem 1. For a given decision $(\boldsymbol{\varphi},\boldsymbol{\pi},\boldsymbol{\omega})\in\boldsymbol{dom}_d$, the SUP $\Theta_n(\boldsymbol{x},\boldsymbol{h},\lambda)$ has an optimal solution at the boundary points ($\overline{\xi}_{ij}$, $\underline{\xi}_{ij}$, $\overline{\delta}_i$ and $\underline{\delta}_i$) or sample points ($\widehat{\xi}_{ij}$ and $\widehat{\delta}_i$) of random variables $\widetilde{\xi}_{ij}$ and $\widetilde{\delta}_i$.

Proof. See Appendix A. □

From Theorem 1, by introducing two sets of auxiliary variables, we can define the following groups of constraints:

$$\widetilde{\delta}_i=\left(\overline{\delta}_i-\widehat{\delta}_i^n\right)\gamma_i^+ +\left(\underline{\delta}_i-\widehat{\delta}_i^n\right)\gamma_i^-+\widehat{\delta}_i^n\ \ \forall i\in N_P$$

$$\widetilde{\xi}_{ij}=\left(\overline{\xi}_{ij}-\widehat{\xi}_{ij}^n\right)\beta_{ij}^+ +\left(\underline{\xi}_{ij}-\widehat{\xi}_{ij}^n\right)\beta_{ij}^-+\widehat{\xi}_{ij}^n\ \ \forall(i,j)\in A$$

$$\gamma_i^+ +\gamma_i^-\leqslant 1\ \ \forall i\in N_P$$

$$\beta_{ij}^{+}+\beta_{ij}^{-}\leqslant 1\ \ \forall(i,j)\in A$$

$$\beta_{ij}^{+},\beta_{ij}^{-}\in\{0,1\}\ \ \forall(i,j)\in A,\ \gamma_i^{+},\gamma_i^{-}\in\{0,1\},\ \forall i\in N_P.$$

In this way, two random variables ($\widetilde{\delta}_i$ and $\widetilde{\xi}_{ij}$) in model (8) can be substituted with their support information (i.e., $\overline{\delta}_i$, $\underline{\delta}_i$, $\overline{\xi}_{ij}$, and $\underline{\xi}_{ij}$), sample values (i.e., $\widehat{\delta}_i^n$ and $\widehat{\xi}_{ij}^n$) and introduced binary auxiliary variables (i.e., β_{ij}^{+}, $\beta_{ij}^{-}\in\{0,1\}$ and $\gamma_i^{+},\gamma_i^{-}\in\{0,1\}$). According to the above derivation, the corresponding bilinear terms $\widetilde{\xi}_{ij}\varphi_{ij}$, $\widetilde{\delta}_i\pi_i$ and $\widetilde{\delta}_i\omega_i$ in (8) can be replaced by the following constraints:

$$\widetilde{\delta}_i\pi_i=\left(\overline{\delta}_i-\widehat{\delta}_i^n\right)\gamma_i^{+}\pi_i+\left(\underline{\delta}_i-\widehat{\delta}_i^n\right)\gamma_i^{-}\pi_i+\widehat{\delta}_i^n\pi_i\ \forall i\in N_P$$

$$\widetilde{\delta}_i\omega_i=\left(\overline{\delta}_i-\widehat{\delta}_i^n\right)\gamma_i^{+}\omega_i+\left(\underline{\delta}_i-\widehat{\delta}_i^n\right)\gamma_i^{-}\omega_i+\widehat{\delta}_i^n\omega_i\ \forall i\in N_P$$

$$\widetilde{\xi}_{ij}\varphi_{ij}=\left(\overline{\xi}_{ij}-\widehat{\xi}_{ij}^n\right)\beta_{ij}^{+}\varphi_{ij}+\left(\underline{\xi}_{ij}-\widehat{\xi}_{ij}^n\right)\beta_{ij}^{-}\varphi_{ij}+\widehat{\xi}_{ij}^n\varphi_{ij}\ \forall(i,j)\in A$$

After the above replacement process, we can finally reformulate each SUP as a mixed-integer (binary) linear programming model by introducing the following Theorem 2.

Theorem 2. Set $\beta_{ij}^{+},\beta_{ij}^{-}\in\{0,1\}$, $\gamma_i^{+},\gamma_i^{-}\in\{0,1\}$, and each SUP is transformed into the mixed-binary linear formulation shown below.

R-1-SUP(n):

$$\Theta_n(\boldsymbol{x},\boldsymbol{h},\lambda)=\max_{\substack{(\boldsymbol{\varphi},\boldsymbol{\pi},\boldsymbol{\omega})\in\boldsymbol{dom}_d,\\ (\Lambda_{ij}^{+},\Lambda_{ij}^{-},u_i^{+},u_i^{-},v_i^{+},v_i^{-})}}\left\{\begin{array}{l}-\sum_{i\in N_D}h_i\pi_i+\sum_{i\in N_R}(SH_i d-h_i)\pi_i+\sum_{i\in N_P}p_i d\pi_i-\sum_{i\in N_R}SH_i\omega_i\\ -\sum_{(i,j)\in A}CAP_{ij}\left[\left(\overline{\xi}_{ij}-\widehat{\xi}_{ij}^n\right)\Lambda_{ij}^{+}+\left(\underline{\xi}_{ij}-\widehat{\xi}_{ij}^n\right)\Lambda_{ij}^{-}+\widehat{\xi}_{ij}^n\varphi_{ij}\right]\\ -\sum_{i\in N_P}p_i d\left[\left(\overline{\delta}_i-\widehat{\delta}_i^n\right)u_i^{+}+\left(\underline{\delta}_i-\widehat{\delta}_i^n\right)u_i^{-}+\widehat{\delta}_i^n\pi_i\right]\\ +\sum_{i\in N_P}p_i\left[\left(\overline{\delta}_i-\widehat{\delta}_i^n\right)v_i^{+}+\left(\underline{\delta}_i-\widehat{\delta}_i^n\right)v_i^{-}+\widehat{\delta}_i^n\omega_i\right]\\ -\lambda\sum_{(i,j)\in A}\left[w_{+}\left(\overline{\xi}_{ij}-\widehat{\xi}_{ij}^n\right)\beta_{ij}^{+}+w_{-}\left(\widehat{\xi}_{ij}^n-\underline{\xi}_{ij}\right)\beta_{ij}^{-}\right]\\ -\lambda\sum_{i\in N_P}\left[w_{+}\left(\overline{\delta}_i-\widehat{\delta}_i^n\right)\gamma_i^{+}+w_{-}\left(\widehat{\delta}_i^n-\underline{\delta}_i\right)\gamma_i^{-}\right]\end{array}\right\}\tag{10a}$$

s.t. (8b)–(8h), and

$$\beta_{ij}^{+}+\beta_{ij}^{-}\leqslant 1\ \forall(i,j)\in A\tag{10b}$$

$$\gamma_i^{+}+\gamma_i^{-}\leqslant 1\ \forall i\in N_P\tag{10c}$$

$$\beta_{ij}^{+},\beta_{ij}^{-}\in\{0,1\}\ \forall(i,j)\in A\tag{10d}$$

$$\gamma_i^{+},\gamma_i^{-}\in\{0,1\}\ \ \forall i\in N_P\tag{10e}$$

$$\Lambda_{ij}^{+}\leqslant M_1^{(i,j)}\beta_{ij}^{+}\ \ \forall(i,j)\in A\tag{10f}$$

$$\Lambda_{ij}^{+}\leqslant\varphi_{ij}\ \forall(i,j)\in A\tag{10g}$$

$$\Lambda_{ij}^{+}\geqslant\varphi_{ij}-M_2^{(i,j)}\left(1-\beta_{ij}^{+}\right)\ \forall(i,j)\in A\tag{10h}$$

$$\Lambda_{ij}^{-}\leqslant M_3^{(i,j)}\beta_{ij}^{-}\ \ \forall(i,j)\in A\tag{10i}$$

$$\Lambda_{ij}^{-}\leqslant\varphi_{ij}\ \ \forall(i,j)\in A\tag{10j}$$

$$\Lambda_{ij}^{-}\geqslant\varphi_{ij}-M_4^{(i,j)}\left(1-\beta_{ij}^{-}\right)\ \ \forall(i,j)\in A\tag{10k}$$

$$\Lambda_{ij}^{+},\Lambda_{ij}^{-}\geqslant 0\ \ \forall(i,j)\in A\tag{10l}$$

$$u_i^{+}\leqslant M_5^{i}\gamma_i^{+}\ \ \forall i\in N_P\tag{10m}$$

$$u_i^{+}\leqslant\pi_i\ \forall i\in N_P\tag{10n}$$

$$u_i^{+}\geqslant\pi_i-M_6^{i}\left(1-\gamma_i^{+}\right)\forall i\in N_P\tag{10o}$$

$$u_i^{-}\leqslant M_7^{i}\gamma_i^{-}\forall i\in N_P\tag{10p}$$

$$u_i^{-}\leqslant\pi_i\forall i\in N_P\tag{10q}$$

$$u_i^{-}\geqslant\pi_i-M_8^{i}\left(1-\gamma_i^{-}\right)\forall i\in N_P\tag{10r}$$

$$u_i^{+},u_i^{-}\geqslant 0\ \ \forall i\in N_P\tag{10s}$$

$$v_i^{+}\leqslant M_9^{i}\gamma_i^{+}\ \ \forall i\in N_P\tag{10t}$$

$$v_i^{+}\leqslant\omega_i\forall i\in N_P\tag{10u}$$

$$v_i^{+}\geqslant\omega_i-M_{10}^{i}\left(1-\gamma_i^{+}\right)\ \forall i\in N_P\tag{10v}$$

$$v_i^{-}\leqslant M_{11}^{i}\gamma_i^{-}\ \ \forall i\in N_P\tag{10w}$$

$$v_i^{-}\leqslant\omega_i\ \ \forall i\in N_P\tag{10x}$$

$$v_i^{-}\geqslant\omega_i-M_{12}^{i}\left(1-\gamma_i^{-}\right)\ \ \forall i\in N_P\tag{10y}$$

$$v_i^{+},v_i^{-}\geqslant 0\ \ \forall i\in N_P\tag{10z}$$

Proof. See Appendix A. □

Remark 2. After going through the decomposition and reformulation process described in **Theorem 1** and **Theorem 2**, our two-stage DRO (5) is finally decomposed into a mixed-integer linear MP (6) and several mixed-binary linear programming SUPs (10). According to the properties of Constraints (8b) to (8h), we can directly set $M_1^{(i,j)}=M_2^{(i,j)}=M_3^{(i,j)}=M_4^{(i,j)}=\max\left\{\max\left\{0,C_i^2-C_{ij1}^1\right\}/Fac_1,\max\left\{0,C_j^3-C_{ij2}^1\right\}/Fac_2\right\}$, $M_5^{i}=M_6^{i}=M_7^{i}=M_8^{i}=C_i^2$, and $M_9^{i}=M_{10}^{i}=M_{11}^{i}=M_{12}^{i}=C_i^3$. At this time, this model can be solved via decomposition algorithms (e.g., the L-shaped method). Mohajerin Esfahani and Kuhn (2018) noted that when the recourse function of a DRO model constructed based on the type-1

Wasserstein ambiguity set can be represented as the piecewise maximum of a finite number of concave functions, then this model can be transformed into a computationally tractable form. Moreover, in the absence of support constraints on the random vector, the two-stage DRO model constructed based on the type-1 Wasserstein ambiguity set is equivalent to a tractable linear programming model (Hanasusanto & Kuhn, 2018). In the event that the polyhedral feasible set of the dual second-stage model is bounded, the two-stage DRO model can be solved by implicitly enumerating the vertices of the feasible set using a column-and-constraint generation algorithm (Saif & Delage, 2021). However, these favorable mathematical properties are not applicable to our FLI-HEP because (*a*) our recourse function is not piecewise concave; (*b*) the random vector in FLI-HEP has a bounded support set; and (*c*) the polyhedral feasible set of the dual second-stage model is unbounded. Therefore, in Section 5, we design an algorithm based on the L-shaped method to achieve an efficient solution of the model.

5. Solution methodology

After the reformulation in the previous section, the DRO model can be solved via decomposition algorithms. Therefore, this section designs two versions of the decomposition algorithm based on the classic L-shaped method. Notably, two-stage SP models can also be solved using similar techniques. In our decomposition algorithm framework, the MP is first solved to obtain a *trial solution* for the preparation-stage model. Next, based on the above trial solution, a group of SUPs (i.e., **R-1-SUP(*n*)**) are solved when the values of the variables in the preparation-stage model are fixed. Then, a series of *cuts* can be obtained by sequentially solving these SUPs. In this section, we consider two methods for generating cuts: single-cut Benders and multi-cut Benders. Finally, these newly generated cuts are added to the MP, which is then solved again. The above iterative steps are repeated until no new cuts can be added by solving the SUPs. In some studies, cuts are divided into *feasible cuts* and *optimal cuts* according to their different functions. The former is responsible for ensuring the feasibility of the primal response-stage model, whereas the latter approximates the optimal objective function value of the primal response-stage model. Since our SUPs are always feasible (see the conclusion proposed in Remark 1 in Section 4.2), feasible cuts are not necessary in our algorithm design process. In the following subsections, Section 5.1 and Section 5.2 introduce our two versions of cuts (i.e., single-cut and multi-cut) added for MP. Section 5.3 introduces several specific acceleration strategies for solving the MP.

5.1. Single-cut Benders for the master problem

In the single-cut Benders, we let parameter t' represent the number of iterations, and the MP can be reformulated as the following model (11) by adding several optimal cuts (11b). Note that cut (11b) is generated based on the dual information provided by **R-1-SUP(*n*)**. After one iteration of the algorithm, a cut can be obtained. The pseudo code is shown in **Algorithm 1**. Let n_1 denote the number of decision variables in the preparation-stage and m_1 denote the number of constraints in the preparation-stage. Similarly, n_2 and m_2 denote the number of decision variables and constraints in the response-stage, respectively. The computational complexity of **Algorithm 1** can be written as $\mathscr{O}\left(t\cdot\left[(n_1+m_1+t')^3+N\cdot(n_2+m_2)^3\right]\right)$.

Algorithm 1: Single-cut version of the algorithm

1: Set $t=0$.
2: Solve the **MP** (11), i.e., model (11). Let $(\boldsymbol{x}^*,\boldsymbol{h}^*,\beta^*)$ be the optimal solution obtained. If $t=0$, then β and the optimal cut is ignored.
3: Set $(\boldsymbol{x}^t,\boldsymbol{h}^t,\beta^t)=(\boldsymbol{x}^*,\boldsymbol{h}^*,\beta^*)$.
4: **For** $n=1$: N **do**
5: Solve **R-1-SUP(*n*)** based on $(\boldsymbol{x}^t,\boldsymbol{h}^t,\beta^t)$. Let $\Theta_n^*(\boldsymbol{x},\boldsymbol{h},\lambda)$ and vector $\left(\pi_i^{t*},\omega_i^{t*},\Lambda_{ij}^{t+*},\Lambda_{ij}^{t-*},\varphi_{ij}^{t*},u_i^{t+*},u_i^{t-*},v_i^{t+*},v_i^{t-*},\beta_{ij}^{t+*},\beta_{ij}^{t-*},\gamma_i^{t+*},\gamma_i^{t-*}\right)^{\mathrm{T}}$ be the optimal objective function value and the optimal solution obtained by solving SUP **R-1-SUP(*n*)**.
6: **End for**
7: Calculate $\mathrm{OBJ}_t=1/N\sum_{n\in[N]}\Theta_n^*(\boldsymbol{x},\boldsymbol{h},\lambda)$.
8: **If** $\mathrm{OBJ}_t\leqslant\beta$ **then**
9: **Break** and the output of model **MP** (11) is an optimal solution.
10: **Else**
11: Set $t=t+1$ and introduce optimal cut (11b) into **MP** (11). **Goto** Line 2.
12: **End if**

(*continued on next column*)

(*continued*)

Single-cut MP:

$$\min_{\substack{(\boldsymbol{x},\boldsymbol{h})\in\boldsymbol{dom}_1,\\ \lambda\geqslant 0,\beta}}\left\{\sum_{i\in N_D\cup N_R}\left(F_i^1x_i+F_i^2h_i\right)+\theta\lambda+\beta\right\} \tag{11a}$$

$$s.t.\ \beta\geqslant\frac{1}{N}\sum_{n\in[N]}\begin{pmatrix}-\sum_{i\in N_D}h_i\pi_i^{t*}+\sum_{i\in N_R}(SH_id-h_i)\pi_i^{t*}+\sum_{i\in N_P}p_id\pi_i^{t*}-\sum_{i\in N_R}SH_i\omega_i^{t*}\\ -\sum_{(i,j)\in A}CAP_{ij}\left[\left(\overline{\xi}_{ij}-\widehat{\xi}_{ij}^n\right)\Lambda_{ij}^{t+*}+\left(\underline{\xi}_{ij}-\widehat{\xi}_{ij}^n\right)\Lambda_{ij}^{t-*}+\widehat{\xi}_{ij}^n\varphi_{ij}^{t*}\right]\\ -\sum_{i\in N_P}p_id\left[\left(\overline{\delta}_i-\widehat{\delta}_i^n\right)u_i^{t+*}+\left(\underline{\delta}_i-\widehat{\delta}_i^n\right)u_i^{t-*}+\widehat{\delta}_i^n\pi_i^{t*}\right]\\ +\sum_{i\in N_P}p_i\left[\left(\overline{\delta}_i-\widehat{\delta}_i^n\right)v_i^{t+*}+\left(\underline{\delta}_i-\widehat{\delta}_i^n\right)v_i^{t-*}+\widehat{\delta}_i^n\omega_i^{t*}\right]\\ -\lambda\sum_{(i,j)\in A}\left[w_+\left(\overline{\xi}_{ij}-\widehat{\xi}_{ij}^n\right)\beta_{ij}^{t+*}+w_-\left(\widehat{\xi}_{ij}^n-\underline{\xi}_{ij}\right)\beta_{ij}^{t-*}\right]\\ -\lambda\sum_{i\in N_P}\left[w_+\left(\overline{\delta}_i-\widehat{\delta}_i^n\right)\gamma_i^{t+*}+w_-\left(\widehat{\delta}_i^n-\underline{\delta}_i\right)\gamma_i^{t-*}\right]\end{pmatrix}\forall t\in[t'] \tag{11b}$$

where $\left(\pi_i^{t*},\omega_i^{t*},\Lambda_{ij}^{t+*},\Lambda_{ij}^{t-*},\varphi_{ij}^{t*},u_i^{t+*},u_i^{t-*},v_i^{t+*},v_i^{t-*},\beta_{ij}^{t+*},\beta_{ij}^{t-*},\gamma_i^{t+*},\gamma_i^{t-*}\right)^{\mathrm{T}}$ is the optimal solution obtained by solving **R-1-SUP(*n*)** at the t^{th} iteration of the algorithm.

5.2. Multi-cut Benders for the master problem

The structure of our SUPs also allows us to extend single-cut Benders to multi-cut versions. In the multi-cut version Benders, we add the following optimal cut (12) to the MP if ρ_n is less than the optimal objective function value of **R-1-SUP(*n*)** for each sample n. The pseudo code of this multi-cut Benders is shown in **Algorithm 2**. The computational complexity of **Algorithm 2** can be written as $\mathscr{O}\left(t\cdot\left[(n_1+m_1+N\cdot t')^3+N\cdot(n_2+m_2)^3\right]\right)$.

Algorithm 2: Multi-cut version of the algorithm

1: Set $t=0$ and *flag* $=0$.
2: Solve the **MP** (with multi-cut), i.e., model (12). Let $(\boldsymbol{x}^*,\boldsymbol{h}^*,\rho_n^*)$ be the optimal solution obtained. If $t=0$, then viewing ρ_n as an unbounded variable and the optimal cut constraint (12b) are ignored.
3: Set $(\boldsymbol{x}^t,\boldsymbol{h}^t,\beta^t)=(\boldsymbol{x}^*,\boldsymbol{h}^*,\rho_n^*)$.
4: **For**$n=1$: N **do**
5: Solve **R-SUP(*n*)** based on **MP** solution $(\boldsymbol{x}^t,\boldsymbol{h}^t,\beta^t)$. Let $\Theta_n^*(\boldsymbol{x},\boldsymbol{h},\lambda)$ and vector $\left(\pi_i^{t*},\omega_i^{t*},\Lambda_{ij}^{t+*},\Lambda_{ij}^{t-*},\varphi_{ij}^{t*},u_i^{t+*},u_i^{t-*},v_i^{t+*},v_i^{t-*},\beta_{ij}^{t+*},\beta_{ij}^{t-*},\gamma_i^{t+*},\gamma_i^{t-*}\right)^{\mathrm{T}}$ be the optimal objective function value obtained by solving SUP **R-SUP(*n*)**.
6: **If** $\Theta_n^*(\boldsymbol{x},\boldsymbol{h},\lambda)\geqslant\rho_n$ **then**
7: Introduce optimal cut (12b) into **MP**.
8: Set *flag* $=1$.
9: **End if**
10: **End for**
11: **If** *flag* $=0$ **then**
12: **Break** and the output of model **MP** (12) is an optimal solution.
13: **Else**

(*continued on next page*)

(*continued*)

14: Set $t = t + 1$, $flag = 0$.
15: **Goto** Line 2.
16: **End if**

Multi-cut MP:

$$\min_{\substack{(\boldsymbol{x},\boldsymbol{h})\in \boldsymbol{dom}_1,\\ \lambda\geqslant 0,\boldsymbol{\rho}}} \left\{ \sum_{i\in N_D\cup N_R} \left(F_i^1 x_i + F_i^2 h_i\right) + \theta\lambda + \frac{1}{N}\sum_{n\in[N]}\rho_n \right\} \tag{12a}$$

$$\begin{aligned} s.t.\ \ \rho_n \geqslant & -\sum_{i\in N_D} h_i \pi_i^{t^*} + \sum_{i\in N_R}(SH_i d - h_i)\pi_i^{t^*} + \sum_{i\in N_P} p_i d\pi_i^{t^*} - \sum_{i\in N_R} SH_i \omega_i^{t^*} \\ & - \sum_{(i,j)\in A} CAP_{ij}\left[\left(\overline{\xi}_{ij} - \widehat{\xi}_{ij}^{\,n}\right)\Lambda_{ij}^{t+^*} + \left(\underline{\xi}_{ij} - \widehat{\xi}_{ij}^{\,n}\right)\Lambda_{ij}^{t-^*} + \widehat{\xi}_{ij}^{\,n}\varphi_{ij}^{t^*}\right] \\ & - \sum_{i\in N_P} p_i d\left[\left(\overline{\delta}_i - \widehat{\delta}_i^{\,n}\right)u_i^{t+^*} + \left(\underline{\delta}_i - \widehat{\delta}_i^{\,n}\right)u_i^{t-^*} + \widehat{\delta}_i^{\,n}\pi_i^{t^*}\right] \\ & + \sum_{i\in N_P} p_i\left[\left(\overline{\delta}_i - \widehat{\delta}_i^{\,n}\right)v_i^{t+^*} + \left(\underline{\delta}_i - \widehat{\delta}_i^{\,n}\right)v_i^{t-^*} + \widehat{\delta}_i^{\,n}\omega_i^{t^*}\right] \\ & - \lambda\sum_{(i,j)\in A}\left[w_+\left(\overline{\xi}_{ij} - \widehat{\xi}_{ij}^{\,n}\right)\beta_{ij}^{t+^*} + w_-\left(\widehat{\xi}_{ij}^{\,n} - \underline{\xi}_{ij}\right)\beta_{ij}^{t-^*}\right] \\ & - \lambda\sum_{i\in N_P}\left[w_+\left(\overline{\delta}_i - \widehat{\delta}_i^{\,n}\right)\gamma_i^{t+^*} + w_-\left(\widehat{\delta}_i^{\,n} - \underline{\delta}_i\right)\gamma_i^{t-^*}\right] \\ & \in [t^{'}], n \in [N] \end{aligned} \qquad \forall t \tag{12b}$$

where $\left(\pi_i^{t^*}, \omega_i^{t^*}, \Lambda_{ij}^{t+^*}, \Lambda_{ij}^{t-^*}, \varphi_{ij}^{t^*}, u_i^{t+^*}, u_i^{t-^*}, v_i^{t+^*}, v_i^{t-^*}, \beta_{ij}^{t+^*}, \beta_{ij}^{t-^*}, \gamma_i^{t+^*}, \gamma_i^{t-^*}\right)^{\mathrm{T}}$ is the optimal solution obtained by solving **SUP(*n*)** at the t^{th} iteration of the algorithm.

Remark 3. Some scholars believe that this multi-cut version is usually more effective when the quantity of historical samples (associated with random variables) is not significantly larger than the quantity of constraints of the preparation-stage model (Birge & Louveaux, 2011). Meanwhile, problems with fewer scenarios are typically solved faster via multi-cut approaches (Bertsimas et al., 2024). Scholars also noted that the relationship between the number of decomposition algorithm iterations and the scale of the MP varies depending on the specific research problem and the number of scenarios (Bertsimas et al., 2024). For example, de Camargo et al. (2008), You and Grossmann (2013), and Birge and Louveaux (2011) all reported mixed results on the performance of these two versions of cuts. Therefore, considering the debate on the applicability of these two types of cuts, we conduct numerical experiments on these two decomposition algorithms in the next section. For a detailed discussion of these two types of cuts, interested readers may refer to Gassmann (1990).

5.3. Acceleration strategy for the master problem

Although we present two versions of **MP** (i.e., (11) or (12)), they are both MIPs, a type of model that is time-consuming to solve using commercial solvers. Therefore, we further provide the following acceleration strategies to improve the efficiency of solving the **MP**.

(1) **Strategy 1**: At each iteration of our proposed algorithm, the **MP** must be solved, which may result in a significant increase in solution time because solving the **MP** is usually time-consuming, especially for large-scale problems. Therefore, to solve the above problem, one possible approach is to apply a branch-and-cut (B&C) scheme. Alternatively, we can also leverage the built-in lazy constraint callback-based implementation of commercial solvers (e.g., CPLEX 12.4 and later versions). In the context of solving an MIP, we can observe that, upon the B&C scheme identifying an incumbent, lazy constraint callback is triggered. This approach allows us to solve the **MP** only once, thereby reducing the computational time needed. Nevertheless, the use of this callback function may not always prove advantageous, as CPLEX disables two other functions (i.e., the dynamic search and the deterministic parallelism) at the same time. For a detailed introduction to this function, interested readers can refer to Dalal and Üster (2018).

(2) **Strategy 2**: When the scale of the problem increases further, another idea is to develop a suitable (meta)heuristic algorithm to obtain a near-optimal solution. Taking the implementation of the genetic algorithm as an example, we can first encode the solution of the **MP** and then implement selection, crossover and mutation operations on the chromosome obtained after encoding. An elite retention strategy can also be further implemented after these operations. Next, the above operations are executed repeatedly until the algorithm termination condition is triggered. Finally, the satisfactory chromosomes obtained by the algorithm are decoded to obtain a satisfactory solution for the **MP**. For interested readers, one may refer to Xin et al. (2023).

6. Numerical experiments

This section describes how our model is applied to the 2010 earthquake that struck Yushu, China (the affected area is shown in Fig. 2). Yushu city is located in Qinghai Province, is situated on the eastern portion of the Tibetan Plateau and encompasses an area of 15,700 square kilometers. Its average elevation above sea level is 4,493.4 m, with the terrain predominantly comprising mountainous plateaus. In 2010, this region experienced 3 earthquakes and more than 10 aftershocks within 5 h, and the earthquakes reached a maximum magnitude of M_w 7.1. Over 1,000 aftershocks occurred in the following two days. A considerable proportion of the residents in the affected areas, some of whom may not have been harmed by the first earthquake, suffered more from subsequent earthquakes and aftershocks. In the event of a disaster, one can see that it is highly important that decision makers are able to coordinate the distribution of relief supplies and the evacuation of evacuees.

In the following sections, we first introduce the parameter settings in Section 6.1. Then, in Section 6.2, we solve different sizes of problems to explore the computing performance of the two decomposition algorithms. In Section 6.3, several sensitivity analyses are performed to explore the impact of considering population evacuation and various parameter changes (e.g., the Wasserstein radius and penalty costs) on the results. Out-of-sample tests are conducted in Section 6.4 to evaluate the robustness of the proposed two-stage model. Section 6.5 provides management insights based on the results. All these numerical experiments are conducted in a commercial solver called GAMS on a personal laptop with a Core Ultra 5-125H CPU and 12 GB of RAM.

6.1. Data description

When setting the parameters in this paper, we refer mainly to the case study of Ni et al. (2018). As illustrated in Fig. 2(b), we investigate an HRLN consisting of 12 nodes and 12 links. We consider the nodes in the inner circle (i.e., nodes 1, 2, 3, 4, 9, and 12) as disaster areas and candidate locations of distribution centers and the nodes in the outer circle (i.e., nodes 5, 6, 7, 8, 10, and 11) as candidate locations of rescue shelters. The distances between different nodes are obtained from the Distance Matrix API (DMAPI) provided by Google. The fixed cost for opening one distribution center (or rescue shelter) and the unit inventory handing cost (i.e., pre-position cost for unit relief supply) are listed in Table 2. Their values are set according to Appendices B.2.1 and B.2.2 of Ni et al. (2018). For the convenience of modeling, we assume that facility location and relief supply pre-position are determined by the same government department. In other words, both types of decisions (i.e., location decisions and pre-position decisions) share the same budget, and we set the government budget for pre-disaster decisions to 200,000. We define a unit of relief supplies as the quantity of relief supplies necessary to sustain one hundred adults for one day (such

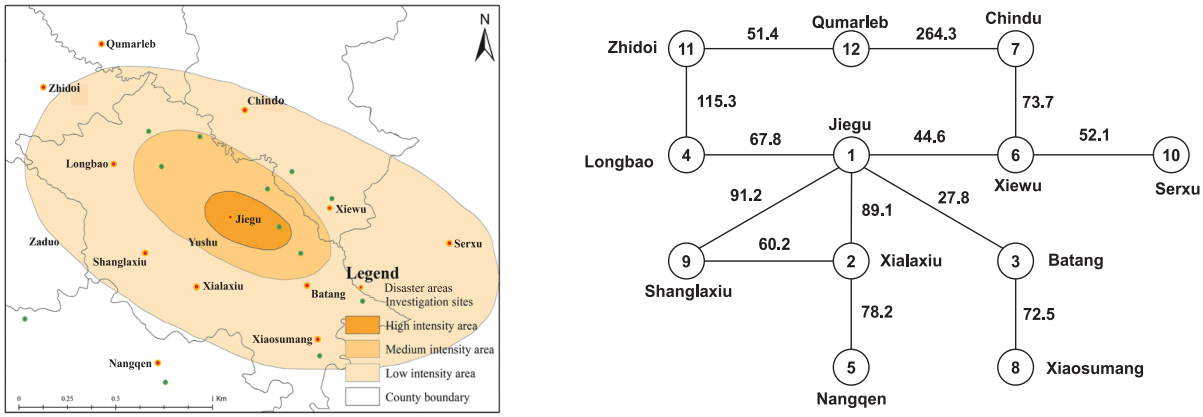

(*a*) The affected area (source: Sun et al. (2019)) (*b*) The HRLN

Fig. 2. The affected area and the HRLN (source: Sun et al. (2019)).

Table 2
Parameter values.

Node	1	2	3	4	5	6	7	8	9	10	11	12
F_i^1	2869	2613	2636	1633	1692	1787	2980	1940	1705	2985	1701	2823
F_i^2	13.06	23.38	12.66	34.65	12.43	24.13	22.95	24.87	14.28	11.71	23.33	11.69

as food and drinking water). From experience, the initial 72-hour period after a disaster is of paramount importance for the implementation of effective relief strategies. Therefore, the total 3-day relief supply requirement is considered a per capita requirement for each affected individual. Then, we determine the proportion of evacuees to the total population (i.e., $\widetilde{\delta}_i$) and the capacity of links (i.e., $\widetilde{\xi}_{ij}$) after the occurrence of the disaster based on local demographics and geography. The population within Yushu is relatively dispersed, the land area is large, and there is a large quantity of mountainous terrain with insufficient road access. Taking the above actual situation into consideration, the total population in each node is randomly generated in the uniform distribution $\mathrm{U}(1500, 2500)$, and the proportion of evacuees to the total population and the post-disaster link capacity in each sample are randomly generated in the distributions $\mathrm{U}(0.3, 0.6)$ and $\mathrm{U}(0.3, 0.5)$. Similar to Ni et al. (2018), we generate a total of 50 sets of samples for the experiment. The maximum relief supply storage at a distribution center or a rescue shelter is set to obey the distribution $\mathrm{U}(800, 1200)$. We next focus on the transportation costs, which are calculated by multiplying the unit cost and distance. Specifically, the transportation cost per meter for one evacuee and unit relief supply is generated from $\mathrm{U}(0.1, 0.2)$ and $\mathrm{U}(0.01, 0.05)$, respectively. The unit penalty cost of the relief shortage on each node follows a uniform distribution in the interval $[4, 6]$. For the penalty cost associated with the failure to evacuate the population, we conduct a number of experiments to determine a value large enough to discourage unmet evacuation demands.

6.2. Model performance

To investigate the model performance, a network with 4 nodes and links (i.e., 4×4) and a network with 12 nodes and links (i.e., 12×12) are considered. We first compare the optimal solutions obtained by the two versions of the algorithm. Table 3 lists the objective value, number of iterations, and selected nodes of each algorithm for the two networks. Judging from the objective functions and solutions obtained by the two approaches, they are basically consistent. Second, we compare the program running times of two different algorithms. To this end, we keep the sizes of both networks constant and gradually change the number of samples. We set the number of samples input to the model from 10 to 80, with an interval of 10. The program running times are reported in Table 4. For both networks, the proposed multi-cut and single-cut decomposition algorithms can obtain optimal solutions in 3,600 s. Therefore, the optimality gap of all the solutions in Table 4 is 0.0 %. We can observe that the multi-cut approach performs better in the simplified network, whereas the single-cut approach calculates faster when the structure of the network is more complex. Therefore, these two methods can be applied to different real-world situations and provide efficient solutions. Third, we discuss the convergence of the two algorithms. As we can see from Fig. 3, the gap between the upper and lower bounds of the two types of algorithms decreases throughout the iteration process, and a smaller gap can be obtained in a relatively short time.

Table 3
Optimal solutions obtained by the two algorithms.

Item	Multi-cut approach		Single-cut approach	
	4×4	12×12	4×4	12×12
Objective value	101373.12	274654.39	101822.47	274045.53
# of iterations	8	50	17	24
Selected nodes	Jiegu (18.7), Xialxiu (46.3), Batang (505.4), Longbao (499.7)	Jiegu (598.5), Batang (835.9), Nangqen (2294.5), Qumarleb (1257.3)	Jiegu (18.4), Xialxiu (46.3), Batang (505.4), Longbao (499.7)	Jiegu (575.6), Batang (830.6), Nangqen (2312.5), Qumarleb (1254.4)

Table 4
Execution times (in seconds) of the proposed approach.

N	Multi-cut approach				Single-cut approach			
	4 × 4	Optimality gap	12 × 12	Optimality gap	4 × 4	Optimality gap	12 × 12	Optimality gap
10	47	0.0 %	184	0.0 %	130	0.0 %	154	0.0 %
20	50	0.0 %	436	0.0 %	135	0.0 %	189	0.0 %
30	154	0.0 %	656	0.0 %	426	0.0 %	496	0.0 %
40	210	0.0 %	1013	0.0 %	593	0.0 %	616	0.0 %
50	269	0.0 %	1616	0.0 %	663	0.0 %	983	0.0 %
60	337	0.0 %	2013	0.0 %	923	0.0 %	985	0.0 %
70	405	0.0 %	2657	0.0 %	1090	0.0 %	2091	0.0 %
80	480	0.0 %	3415	0.0 %	1110	0.0 %	2666	0.0 %

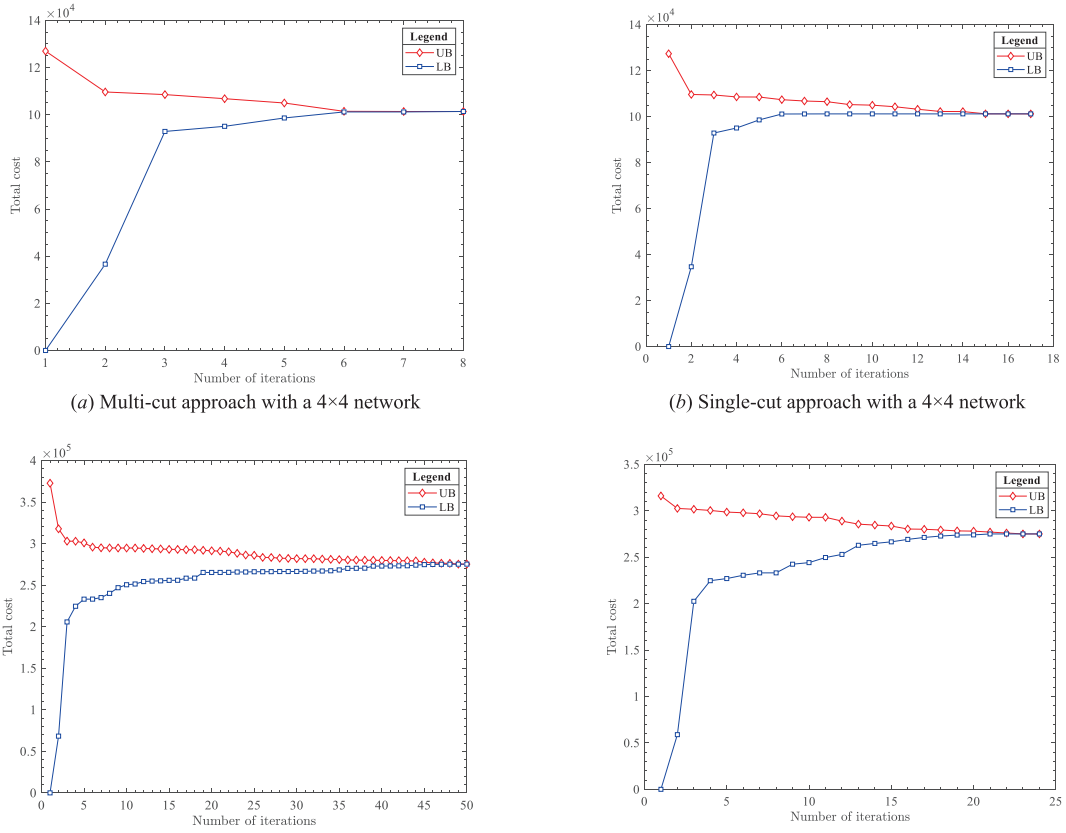

(*a*) Multi-cut approach with a 4×4 network

(*b*) Single-cut approach with a 4×4 network

(*c*) Multi-cut approach with a 12×12 network

(*d*) Single-cut approach with a 12×12 network

Fig. 3. Convergence of the multi-cut and single-cut approaches.

Table 5
Comparisons of models with and without evacuation planning.

Calculation indicators	Model with evacuation planning (our model)	Model without evacuation planning
Average out-of-sample total cost	277219.5	283105.4
Maximum out-of-sample total cost	289138.8	294025.7
Minimum out-of-sample total cost	265517.8	274677.2
Quantity of relief supplies	4986.0	4422.8
Opening facilities	Xialaxiu, Nangqen, Xiewu, Xiaosumang, Shanglaxiu, Zhidoi, Qumarleb	Batang, Nangqen, Serxu, Qumarleb

6.3. Computational results and sensitivity analysis

6.3.1. Effect of considering evacuees

We further conduct several experiments to investigate the effect of considering evacuees in the network. To this end, we obtain the optimal solutions of the preparation-stage model without considering evacuees and then institute it into the response-stage of the proposed model to obtain the out-of-sample total cost. After the above operations, we obtain the results shown in Table 5.

Interestingly, when we do not consider the evacuation planning factor, the out-of-sample total cost increases. The reason for this change is that the opening of a facility necessitates the fulfillment of its minimum relief supply storage requirements. When considering evacuation planning, more relief shelters are opened, allowing some relief supplies to be located where transportation costs could be reduced. This means that a decentralized pre-position relief supply model can reduce regional transportation costs. In terms of the quantity of relief supplies and the opening of facilities, our model attempts to open more facilities and pre-

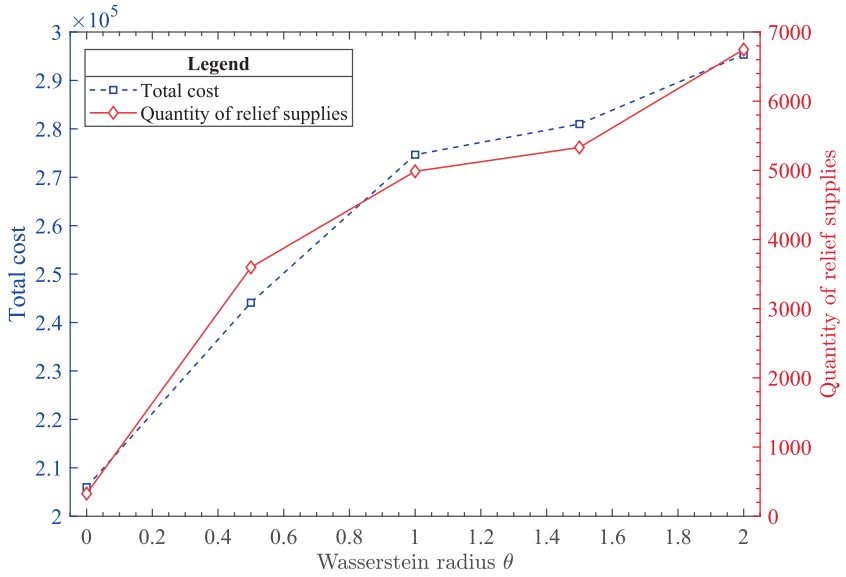

Fig. 4. Total cost and quantity of relief supplies under different Wasserstein radii θ.

position more relief supplies than does the case without considering evacuees. The above situation is in line with our expectations. Evacuees need rescue shelters to provide them with survival guarantees. The presence of evacuees will inevitably lead decision makers to choose to increase the number of open facilities and the storage of relief supplies. These results demonstrate the importance and necessity of simultaneous consideration of the transportation of relief supplies as well as evacuation planning in HRLN design.

6.3.2. *Sensitivity analysis for the Wasserstein radius*

In this subsection, we conduct extensive experiments under various Wasserstein radii to analyze the effect of the degree of uncertainty. We create different scenarios by setting the radius θ in the interval $[0, 2]$. Specifically, our model reduces to a deterministic model when we set the value of θ to 0. Fig. 4 illustrates the changes in the total cost and quantity of relief supplies pre-positioned under different scenarios (i.e., Wasserstein radius). One can observe that there is a significant increase in the optimal value of the model as the radius θ increases, along with an increase in the quantity of pre-positioned relief supplies. In particular, the total cost paid by the decision maker increases by approximately 50 % as θ changes from 0 to 2. The change in the quantity of pre-positioned relief supplies is even more dramatic, as it increases by more than 10 times (from close to 600 to more than 6,000). In contrast to the deterministic scenario (i.e., scenario θ equals 0), we find that as the uncertainty (radius θ) expands, the solution to the problem becomes more conservative. This observation also indicates that a lack of awareness of uncertainty may have significant consequences. It is evident that a relief supply pre-positioning scheme when θ is assumed to be 0 will be unable to cope with a disaster situation when θ is assumed to be a value other than 0, such as 1 or 2. This ignorance could lead to a supply gap during pre-disaster preparation. However, if too much relief supply is pre-positioned, it will cause redundancy and waste of resources. Therefore, the value of θ should not be set as large as possible. The decision maker needs to be careful in determining the value of θ because it can

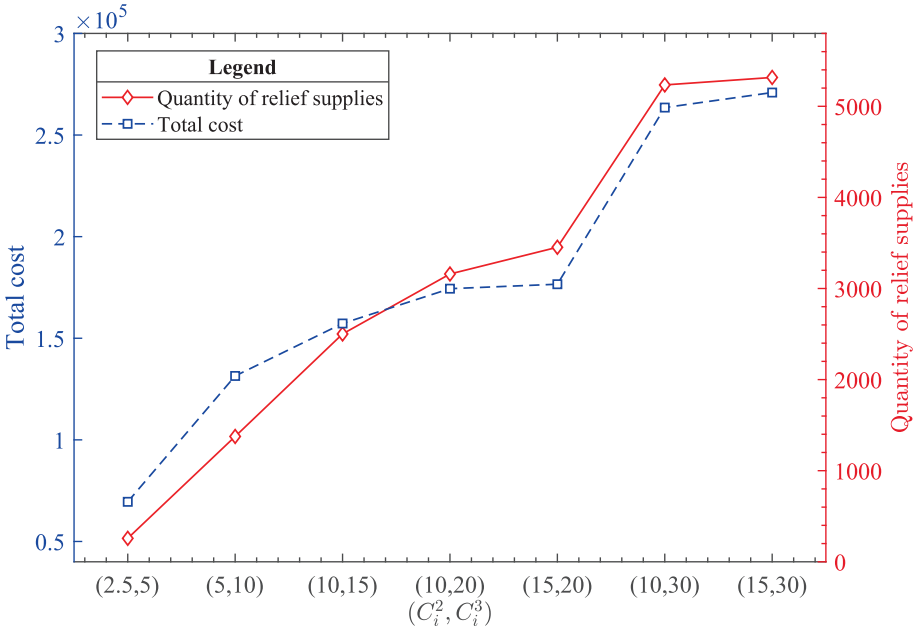

Fig. 5. Impact of penalty cost for unmet relief and evacuee demand.

Table 6
Nodes selected under different penalty cost settings.

(C_i^2, C_i^3)	Node(s)
(2.5, 5)	Qumarleb
(5, 10)	Nangqen, Xiwwu
(10, 15)	Nangqen, Chindu, Xiaosumang
(10, 20)	Xialaxiu, Chindu, Xiaosumang, Zhidoi
(15, 20)	Nangqen, Xiaosumang, Serxu, Zhidoi
(10, 30)	Xialaxiu, Nangqen, Xiewu, Xiaosumang, Shanglaxiu, Zhidoi, Qumarleb
(15, 30)	Batang, Nangqen, Xiewu, Chindu, Shanglaxiu, Serxu, Qumarleb

lead to an over-conservatism decision when θ is large.

6.3.3. Sensitivity analysis for unit penalty cost

This section further discusses the impact of the unit penalty cost on the optimal solutions. To this end, we conduct numerical experiments with different unit penalty costs (C_i^2, C_i^3) for relief supply shortages and failures to evacuate populations under seven different scenarios, i.e., $\{(2.5,5),(5,10),(10,15),(10,20),(15,20),(10,30),(15,30)\}$. We use Fig. 5 and Table 6 to report the results under seven scenarios, and we can observe that the total cost, quantity of relief supplies pre-positioned, and number of facilities opened increase as the value of the unit penalty cost increases. This suggests that when the impact of unmet demands for relief supplies and evacuees is greater, decision makers tend to be more conservative in their decisions. In other words, there may be serious consequences during the corresponding stage of a disaster if decision makers are not fully cognizant of the impact of unmet demands. When the unit penalty cost is low (e.g., $(C_i^2, C_i^3) = (2.5,5)$), we find that decision makers will only open a facility that is pre-positioned with less than 700 units of relief supply. However, a very large quantity of relief supply demand (over 4,000 units) is not met, in contrast to when (C_i^2, C_i^3) is greater than $(10,30)$. This observation implies that the magnitude of unit penalty costs is crucial, as lower costs results in insufficient relief supplies and a smaller number of facilities opened, which may ultimately lead to an increased number of casualties. Conversely, a higher value may result in the waste of supplies. Moreover, it is worth noting that there are some clear thresholds for the impact of unit penalty costs. Fig. 5 clearly shows two characteristics. First, when (C_i^2, C_i^3) increases from $(10,20)$ to $(15,20)$, neither the solution of the model nor the value of the objective function significantly changes. However, as (C_i^2, C_i^3) continues to grow, a dramatic increase in total cost, the quantity of relief supplies, and the number of facilities opened can be found. Second, after $(C_i^2, C_i^3) \geqslant (10,30)$, the changes in the total cost, quantity of relief supplies, and number of facilities opened remain stable. Considering the parameter settings, the decision maker should set the value of the unit penalty cost to $(10,30)$ since it is a reliable choice. Meanwhile, higher value settings are unable to deliver substantial improvements.

6.4. Out-of-sample analysis

In this subsection, we conduct several out-of-sample tests to investigate the out-of-sample performance of our model. Specifically, we construct the samples of $\tilde{\zeta}$ on the basis of distribution $U(\mu - \kappa\sigma, \mu + \kappa\sigma)$, where μ and σ are the mean and standard deviation, respectively, as stated in Section 6.1, and where $\kappa \geqslant 0$ is a scale parameter to control the uncertainty. We generate 1,000 samples for each of the three scenarios with $\kappa = 1$, 1.5, and 2 and substitute the optimal solution of the original model into the response-stage model to resolve it, obtain the out-of-sample total cost (see Fig. 6(*a*)) and calculate the out-of-sample disappointment (refer to *DIS*, see Fig. 6(*b*)) on the basis of Wang et al. (2023). This indicator is used to indicate the difference between the cost required to implement an optimal decision and the estimated cost. The calculation method of this indicator is shown in Equation (13).

$$DIS = \max\left\{\frac{OPC - MOC}{MOC}, 0\right\} \times 100\% \tag{13}$$

where *OPC* and *MOC* denote the out-of-sample cost and optimal cost, respectively.

We find that in the context of different distribution functions, as parameter κ changes (i.e., the degree of uncertainty increases), the actual out-of-sample cost generated is concentrated. We show the out-of-sample total cost under different scenarios in Table 7. As the parameter κ increases, the increase in total cost is relatively stable (approximately 10 %). In terms of out-of-sample disappointment, our proposed model can always control the disappointment indicator *DIS* within a reasonable range. In most cases, the *DIS* is within 10 %. The above experimental results prove that the out-of-sample performance of our proposed model is satisfactory.

Table 7
Average, maximum and minimum out-of-sample total costs.

Case	$\kappa = 1$	$\kappa = 1.5$	$\kappa = 2$
Average	277219.5	291632.7	305281.6
Maximum	289138.8	307813.1	334679.3
Minimum	265517.8	269447.8	275675.2

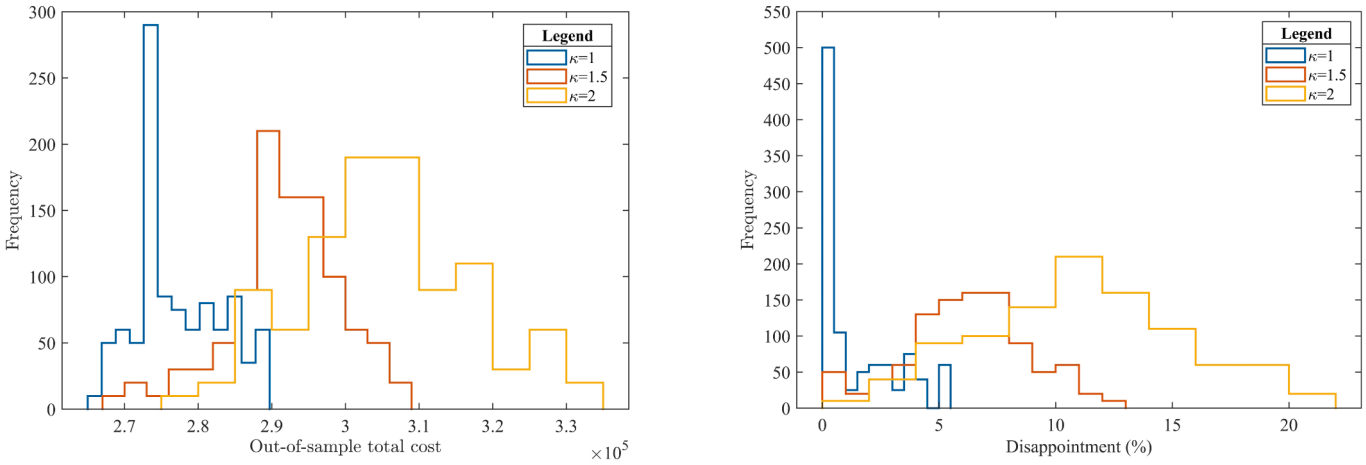

(*a*) Out-of-sample total cost (*b*) Disappointment value

Fig. 6. Out-of-sample results with $\kappa = 1$, $\kappa = 1.5$, and $\kappa = 2$.

Table 8
Average, maximum and minimum disappointment values of the two models.

Item	Our model (5)	SP model with SAA
Maximum	4.60 %	6.08 %
Minimum	0.00 %	0.00 %
Average	0.93 %	1.22 %
90^{th} percentile	3.11 %	4.11 %
95^{th} percentile	3.71 %	4.89 %

In addition, through out-of-sample analysis, we can also compare our method with common modeling methods (e.g., stochastic programming). To this end, we set parameter $\kappa = 1$ and generate 1,000 samples and use them as inputs for the two-stage DRO model (5) and two-stage SP model (i.e., (1) to (2)). We then calculate the out-of-sample disappointment values of the two models. For the 1,000 disappointment values corresponding to each model, we calculate their maximum, minimum, average, 90^{th} percentile and 95^{th} percentile. These values are reported in Table 8. Table 8 shows that, except for the minimum disappointment value corresponding to the two models, model (5) is better in all other indicators. This means that, compared with the SP model, our DRO model has better out-of-sample performance. This is because when faced with various simulated scenarios, the actual costs incurred when implementing our model's solutions are generally lower than those of the SP model.

Finally, we explore the reasonable value of the Wasserstein radius in Section 6.3.2. Here, we still set parameter $\kappa = 1$ and generate 1,000 samples. We solve our model (5) and conduct 10 experiments by setting θ between 0.2 and 2 with a step size of 0.2. Using the solutions obtained from the 10 experiments and the 1,000 samples generated, we can calculate 1000 out-of-sample disappointment values for each θ. The maximum, minimum, average, 90^{th} percentile and 95^{th} percentile values of these disappointment values for each θ are shown in Fig. 7. Overall, as θ increases, all the indicators gradually decrease. This is because θ is a parameter that controls the size of the ambiguity set. As it increases, the obtained solutions become less conservative. Considering Fig. 7 and the costs shown in Fig. 4, we believe that the decision maker can set θ to 0.8. At this point, the cost to decision makers is not high, and the model also shows good out-of-sample performance.

6.5. Managerial insights

This subsection discusses the managerial insights from our model and solution methodology based on the above numerical experiments.

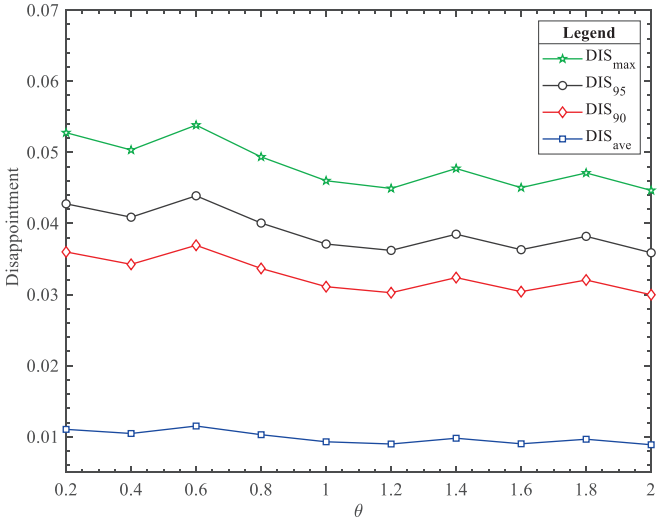

Fig. 7. Disappointment values of our model with different θ.

- Our proposed model and algorithm can provide useful decision tools for the design of HRLNs while considering uncertainty for decision makers in government emergency response sectors. The uncertainty of disaster occurrence and the lack of relevant historical data have created many challenges for decision makers in making disaster prevention decisions. When aware of the uncertainty of a disaster, decision makers can develop target schemes for emergency facility locations, relief supply pre-position, affected population evacuation, and relief supply distribution based on our model. For example, by studying the calculation results in Section 6.3.1, decision makers can obtain a better understanding of the relationship between the degree of uncertainty and the optimal solutions and formulate realistic policies accordingly.
- This paper illustrates the importance of simultaneously considering two types of flow in the design of HRLNs. On the one hand, both types of flows will crowd out the same, scarce infrastructure capacity (i.e., road capacity). On the other hand, the flow of evacuees in the HRLN affects the direction of the relief supply flow because evacuees also need relief supplies. Decision makers should understand the conflicts between relief supply flow and evacuee flow at the response-stage and take them into account in decision-making frameworks. This idea plays a critical role in mitigating road congestion that may occur after a disaster. Meanwhile, the evacuation of the transfer population leads to a shift in the location of the relief supply demand, which is a more realistic consideration that our model can bring to the table.
- The setting of penalty costs for unmet relief supply demands and evacuation demands requires careful consideration. The location and number of facilities, as well as schemes for transporting relief supplies and evacuees, are strongly influenced by the penalty cost. Decision makers can achieve trade-offs between different objectives by analyzing the relationships between unit penalty costs, total costs and quantities of pre-positioned relief supplies.
- The solution approaches are designed to provide various options for HRLNs of different sizes. Our proposed multi-cut and single-cut versions perform well with different sizes of nodes and links. Therefore, in realistic applications, a suitable method for solving the problem can be selected according to the actual problem size.

7. Conclusion

The high uncertainty of natural disasters (e.g., time uncertainty and spatial uncertainty) has led to booming research on the design of humanitarian relief logistics networks (HRLNs). In the actual implementation of relief activities, both the supply of relief supplies and the evacuation of evacuees inevitably utilize fragile logistics infrastructure, such as roads. Nevertheless, the majority of existing research has concentrated on a single area of study, resulting in the emergence of two research paradigms, i.e., supply-centric (focused on the transportation of relief supplies) and beneficiary-centric (focused on the transportation of evacuees) paradigms. Motivated by the above background, we consider the integration of the three types of decisions that are of interest to decision makers when conducting HRLN design, i.e., emergency facility (i.e., distribution centers and relief shelters) location, relief inventory pre-positioning, and human evacuation planning. With the help of the advanced distributionally robust optimization (DRO) technique, we model this integrated decision-making problem as a two-stage DRO model. Each stage of our model involves decisions for pre- and post-disaster periods. We use the type-1 Wasserstein metric to construct an ambiguity set to describe the distribution function of uncertain parameters in the model (i.e., the number of evacuees and the road capacity). To solve the above model, we design two customized decomposition algorithms (i.e., single-cut and multi-cut versions) based on the classical L-shaped algorithm. In addition, several numerical experiments on the Yushu earthquake in China are carried out to verify the effectiveness of the DRO model and algorithms.

The results show that the proposed two-stage DRO model, which considers both the relief supply flow and the evacuee flow, can provide critical managerial insights for decision makers. First, we illustrate the effect of considering evacuee flow in the design of humanitarian logistics networks. Obviously, the transport of the transfer population (i.e., evacuee) and relief supply creates conflicts in the use of infrastructure (i.e., road capacity). Moreover, the implementation of evacuation planning can also cause changes in the demand for relief supplies at different nodes. Numerical experiments show that models that do not consider evacuation planning result in higher total costs. Second, we analyze the location and transport schemes under different scales of uncertainty. The conclusions obtained can help decision makers reach reliable and efficient solutions in the preparation and response-stages under different uncertainties. Third, we discuss the relationship between the penalty cost and the total cost and quantity of pre-positioned relief supplies. Two thresholds are clearly found for the effect of penalty costs on the optimal solution. This finding can provide advice to decision makers on the trade-off between effectiveness and cost objectives. Finally, the out-of-sample analyses carried out show that our model and algorithm have favorable out-of-sample performance and are able to combat various uncertainty scenarios well. There is at most a 20 % variation in total costs among all distribution scenarios.

Future studies can consider more relief supply distribution modes, such as adding drone transportation to our model framework. The ability to collect real-world data as much as possible to verify the effectiveness of the model and the algorithm is also a research idea. In addition, considering fairness constraints in the model framework to achieve a fair distribution of the relief supply and introducing risk indicators to obtain risk-averse solutions are also interesting research directions.

CRediT authorship contribution statement

Tao Zhang: Writing – review & editing, Writing – original draft, Visualization, Software, Methodology, Investigation, Data curation, Conceptualization. **Shuaian Wang:** Writing – review & editing, Writing – original draft, Visualization, Methodology, Formal analysis, Conceptualization. **Xu Xin:** Writing – review & editing, Writing – original draft, Validation, Supervision, Methodology, Investigation, Funding acquisition, Formal analysis, Conceptualization.

Declaration of competing interest

The authors declare that they have no known competing financial interests or personal relationships that could have appeared to influence the work reported in this paper.

Acknowledgments

The authors would like to express their gratitude for the support provided by the National Natural Science Foundation of China [Grant numbers 72371221 and 72504206], and the Research Grants Council of the Hong Kong Special Administrative Region, China [Project number HKSAR RGC TRS T32-707/22-N].

Appendix A:. Proofs of Theorems

Proof of Theorem 1. **Proof.** For a given $(\boldsymbol{x}, \boldsymbol{h}, \lambda)$, function $\Theta_n(\boldsymbol{x}, \boldsymbol{h}, \lambda)$ can be expressed as:

$$\Theta_n(\boldsymbol{x}, \boldsymbol{h}, \lambda) = \max_{\widetilde{\zeta} \in \Xi} \{ g_d(\boldsymbol{x}, \boldsymbol{h}, \widetilde{\zeta}) - \lambda \mathrm{dis}(\widetilde{\zeta}, \widehat{\zeta}^n) \} \tag{A1}$$

Then, according to the definition of $\mathrm{dis}(\widetilde{\zeta}, \widehat{\zeta}^n)$, we can derive

$$\mathrm{dis}(\widetilde{\zeta}, \widehat{\zeta}^n) = \mathrm{dis}\left(\left(\widetilde{\xi}_{ij}, \widetilde{\delta}_i \right), \left(\widehat{\xi}_{ij}^n, \widehat{\delta}_i^n \right) \right)$$

$$= \sum_{(i,j) \in A} \max \left\{ \boldsymbol{w}_+ \left(\widetilde{\xi}_{ij} - \widehat{\xi}_{ij}^n \right), \boldsymbol{w}_- \left(\widehat{\xi}_{ij}^n - \widetilde{\xi}_{ij} \right) \right\} + \sum_{i \in N_P} \max \left\{ \boldsymbol{w}_+ \left(\widetilde{\delta}_i - \widehat{\delta}_i^n \right), \boldsymbol{w}_- \left(\widehat{\delta}_i^n - \widetilde{\delta}_i \right) \right\}.$$

For all $\widetilde{\xi}_{ij}$, there exist two cases, i.e., $\widetilde{\xi}_{ij} \leqslant \widehat{\xi}_{ij}^n$ and $\widetilde{\xi}_{ij} \geqslant \widehat{\xi}_{ij}^n$. The function $\Theta_n(\boldsymbol{x}, \boldsymbol{h}, \lambda)$ is a linear function associated with $\widetilde{\xi}_{ij}$. Thus, an optimal value of $\widetilde{\xi}_{ij}$ is obtained at $\widetilde{\xi}_{ij} = \widehat{\xi}_{ij}^n$ or $\underline{\xi}_{ij}$ for the first case and $\widetilde{\xi}_{ij} = \widehat{\xi}_{ij}^n$ or $\overline{\xi}_{ij}$ for the second case. Therefore, there must be $\widetilde{\xi}_{ij} = \widehat{\xi}_{ij}^n$, $\overline{\xi}_{ij}$, or $\underline{\xi}_{ij}$ in an optimal solution of function $\Theta_n(\boldsymbol{x}, \boldsymbol{h}, \lambda)$. (Q.E.D.).

Proof of Theorem 2. **Proof.** Without loss of generality, we first focus on the bilinear term $\widetilde{\xi}_{ij}\varphi_{ij}$. The reformulations of the other bilinear terms are similar. Note that there are still bilinear terms $\beta_{ij}^+\varphi_{ij}$ and $\beta_{ij}^-\varphi_{ij}$ associated with φ_{ij}, so we introduce two variables, Λ_{ij}^+ and Λ_{ij}^-. Then, we let term $\left(\overline{\xi}_{ij} - \widehat{\xi}_{ij}^n\right)\Lambda_{ij}^+ + \left(\underline{\xi}_{ij} - \widehat{\xi}_{ij}^n\right)\Lambda_{ij}^- + \widehat{\xi}_{ij}^n\varphi_{ij}$ replace term $\widetilde{\xi}_{ij}\varphi_{ij}$ in the model and add the following constraints:

$$\Lambda_{ij}^+ \leqslant M\beta_{ij}^+ \forall (i,j) \in A \tag{A2}$$

$$\Lambda_{ij}^+ \leqslant \varphi_{ij}^1 \forall (i,j) \in A \tag{A3}$$

$$\Lambda_{ij}^+ \geqslant \varphi_{ij}^1 - M\left(1 - \beta_{ij}^+\right) \forall (i,j) \in A \tag{A4}$$

$$\Lambda_{ij}^- \leqslant M\beta_{ij}^- \forall (i,j) \in A \tag{A5}$$

$$\Lambda_{ij}^- \leqslant \varphi_{ij}^1 \forall (i,j) \in A \tag{A6}$$

$$\Lambda_{ij}^- \geqslant \varphi_{ij}^1 - M\left(1 - \beta_{ij}^-\right) \forall (i,j) \in A \tag{A7}$$

$$\Lambda_{ij}^{+}, \Lambda_{ij}^{-} \geqslant 0 \forall (i,j) \in A \tag{A8}$$

where M is a sufficiently large positive number.

Similarly, by applying the same techniques to $\widetilde{\delta}_i \pi_i$ and $\widetilde{\delta}_i \omega_i$, we can derive the mixed-integer (binary) linear formulation proposed in Theorem 2. (Q.E.D.).

Data availability

Data will be made available on request.

References

Baron, O., Milner, J., Naseraldin, H., 2011. Facility location: a robust optimization approach. Prod. Oper. Manag. 20 (5), 772–785.

Bertsimas, D., Cory-Wright, R., Pauphilet, J., Petridis, P., 2024. A stochastic Benders decomposition scheme for large-scale stochastic network design. INFORMS J. Comput.

Bertsimas, D., Thiele, A., 2006. A robust optimization approach to inventory theory. Oper. Res. 54 (1), 150–168.

Besiou, M., Pedraza-Martinez, A. J., & Van Wassenhove, L. N. (2018). OR applied to humanitarian operations. In (Vol. 269, pp. 397–405): Elsevier.

Birge, J.R., Louveaux, F., 2011. *Introduction to stochastic programming*. Springer Science & Business Media.

Che, A., Li, J., Chu, F., Chu, C., 2024. Optimizing emergency supply pre-positioning for disaster relief: a two-stage distributionally robust approach. Comput. Oper. Res. 166, 106607.

Chu, J.C., Chen, S.-C., 2016. Optimization of transportation-infrastructure-system protection considering weighted connectivity reliability. J. Infrastruct. Syst. 22 (1), 04015008.

Dalal, J., Üster, H., 2018. Combining worst case and average case considerations in an integrated emergency response network design problem. Transp. Sci. 52 (1), 171–188.

Dalal, J., Üster, H., 2021. Robust emergency relief supply planning for foreseen disasters under evacuation-side uncertainty. Transp. Sci. 55 (3), 791–813.

de Camargo, R.S., Miranda Jr, G., Luna, H.P., 2008. Benders decomposition for the uncapacitated multiple allocation hub location problem. Comput. Oper. Res. 35 (4), 1047–1064.

El Tonbari, M., Nemhauser, G., Toriello, A., 2024. Distributionally robust disaster relief planning under the Wasserstein set. Comput. Oper. Res. 106689.

Erbeyoğlu, G., Bilge, Ü., 2020. A robust disaster preparedness model for effective and fair disaster response. Eur. J. Oper. Res. 280 (2), 479–494.

Fan, X., Juang, C.H., Wasowski, J., Huang, R., Xu, Q., Scaringi, G., van Westen, C.J., Havenith, H.-B., 2018. What we have learned from the 2008 Wenchuan Earthquake and its aftermath: a decade of research and challenges. Eng. Geol. 241, 25–32.

Gao, R., Kleywegt;, A., 2023. Distributionally robust stochastic optimization with Wasserstein distance. Math. Oper. Res. 48 (2), 603–655.

Gassmann, H.I., 1990. MSLiP: a computer code for the multistage stochastic linear programming problem. Math. Program. 47, 407–423.

Gupta, S., Starr, M.K., Farahani, R.Z., Matinrad, N., 2016. Disaster management from a POM perspective: Mapping a new domain. Prod. Oper. Manag. 25 (10), 1611–1637.

Hanasusanto, G.A., Kuhn, D., 2018. Conic programming reformulations of two-stage distributionally robust linear programs over wasserstein balls. Oper. Res. 66 (3), 849–869.

Hao, Z., He, L., Hu, Z., Jiang, J., 2020. Robust vehicle pre-allocation with uncertain covariates. Prod. Oper. Manag. 29 (4), 955–972.

Ho-Nguyen, N., Kılınç-Karzan, F., Küçükyavuz, S., Lee, D., 2022. Distributionally robust chance-constrained programs with right-hand side uncertainty under Wasserstein ambiguity. Math. Program. 196 (1), 641–672.

Jin, Z., Ng, K.K., Zhang, C., Liu, W., Zhang, F., Xu, G., 2024. A risk-averse distributionally robust optimisation approach for drone-supported relief facility location problem. Transport. Res. Part e: Log. Transport. Rev. 186, 103538.

Kazama, M., Noda, T., 2012. Damage statistics (Summary of the 2011 off the Pacific Coast of Tohoku Earthquake damage). Soils Found. 52 (5), 780–792.

Liu, K., Li, Q., Zhang, Z.-H., 2019. Distributionally robust optimization of an emergency medical service station location and sizing problem with joint chance constraints. Transp. Res. B Methodol. 119, 79–101.

Liu, M., Lai, K.-H., Wong, C.W.Y., Xin, X., Lun, V.Y.H., 2025. Smart ports for sustainable shipping: concept and practices revisited through the case study of China's Tianjin port. Maritime Econ. Log. 27 (1), 50–95.

Mohajerin Esfahani, P., Kuhn, D., 2018. Data-driven distributionally robust optimization using the Wasserstein metric: performance guarantees and tractable reformulations. Math. Program. 171 (1), 115–166.

Ng, M., Waller, S.T., 2010. Reliable evacuation planning via demand inflation and supply deflation. Transport. Res. Part e: Log. Transport. Rev. 46 (6), 1086–1094.

Ni, W., Shu, J., Song, M., 2018. Location and emergency inventory pre-positioning for disaster response operations: Min-max robust model and a case study of Yushu earthquake. Prod. Oper. Manag. 27 (1), 160–183.

Noham, R., Tzur, M., 2018. Designing humanitarian supply chains by incorporating actual post-disaster decisions. Eur. J. Oper. Res. 265 (3), 1064–1077.

Noyan, N., 2012. Risk-averse two-stage stochastic programming with an application to disaster management. Comput. Oper. Res. 39 (3), 541–559.

Özdamar, L., Demir, O., 2012. A hierarchical clustering and routing procedure for large scale disaster relief logistics planning. Transport. Res. Part e: Log. Transport. Rev. 48 (3), 591–602.

Pouraliakbari-Mamaghani, M., Saif, A., Kamal, N., 2023. Reliable design of a congested disaster relief network: a two-stage stochastic-robust optimization approach. Socioecon. Plann. Sci. 86, 101498.

Rambha, T., Nozick, L.K., Davidson, R., Yi, W., Yang, K., 2021. A stochastic optimization model for staged hospital evacuation during hurricanes. Transport. Res. Part e: Log. Transport. Rev. 151, 102321.

Rawls, C.G., Turnquist, M.A., 2010. Pre-positioning of emergency supplies for disaster response. Transp. Res. B Methodol. 44 (4), 521–534.

Recchiuto, C.T., Sgorbissa, A., 2018. Post-disaster assessment with unmanned aerial vehicles: a survey on practical implementations and research approaches. J. Field Rob. 35 (4), 459–490.

Sabbaghtorkan, M., Batta, R., He, Q., 2020. Prepositioning of assets and supplies in disaster operations management: Review and research gap identification. Eur. J. Oper. Res. 284 (1), 1–19.

Saif, A., Delage, E., 2021. Data-driven distributionally robust capacitated facility location problem. Eur. J. Oper. Res. 291 (3), 995–1007.

Salmerón, J., Apte, A., 2010. Stochastic optimization for natural disaster asset prepositioning. Prod. Oper. Manag. 19 (5), 561–574.

Shahparvari, S., Chhetri, P., Abbasi, B., Abareshi, A., 2016. Enhancing emergency evacuation response of late evacuees: Revisiting the case of Australian Black Saturday bushfire. Transport. Res. Part e: Log. Transport. Rev. 93, 148–176.

Smith, J.E., Winkler, R.L., 2006. The optimizer's curse: Skepticism and postdecision surprise in decision analysis. Manag. Sci. 52 (3), 311–322.

Stauffer, J.M., Kumar, S., 2021. Impact of incorporating returns into pre-disaster deployments for rapid-onset predictable disasters. Prod. Oper. Manag. 30 (2), 451–474.

Sun, L., Su, G., Tian, Q., Qi, W., Liu, F., Qi, M., Li, R., 2019. Religious belief and Tibetans' response to earthquake disaster: a case study of the 2010 Ms 7.1 Yushu earthquake, Qinghai Province, China. Nat. Hazards 99, 141–159.

Tofighi, S., Torabi, S.A., Mansouri, S.A., 2016. Humanitarian logistics network design under mixed uncertainty. Eur. J. Oper. Res. 250 (1), 239–250.

Wang, D., Yang, K., Yang, L., Dong, J., 2023. Two-stage distributionally robust optimization for disaster relief logistics under option contract and demand ambiguity. Transport. Res. Part e: Log. Transport. Rev. 170, 103025.

Wang, D., Yang, K., Yuen, K.F., Yang, L., Dong, J., 2024. Hybrid risk-averse location-inventory-allocation with secondary disaster considerations in disaster relief logistics: a distributionally robust approach. Transport. Res. Part e: Log. Transport. Rev. 186, 103558.

Wang, J., Cai, J., Yue, X., Suresh, N.C., 2021. Pre-positioning and real-time disaster response operations: Optimization with mobile phone location data. Transport. Res. Part e: Log. Transport. Rev. 150, 102344.

Xin, X., Wang, S., Zhang, T., 2025. Truck-drone supported humanitarian relief logistics network design: a two-stage distributionally robust optimization approach. Transp. Res. Part C Emerging Technol. 178, 105231.

Xin, X., Wang, X., Zhang, T., Chen, H., Guo, Q., Zhou, S., 2023. Liner alliance shipping network design model with shippers' choice inertia and empty container relocation. Electron. Res. Arch. 31 (9), 5509–5540.

Ye, Y., Jiao, W., Yan, H., 2020. Managing relief inventories responding to natural disasters: Gaps between practice and literature. Prod. Oper. Manag. 29 (4), 807–832.

Yin, Y., Wang, J., Chu, F., Wang, D., 2024a. Distributionally robust multi-period humanitarian relief network design integrating facility location, supply inventory and allocation, and evacuation planning. Int. J. Prod. Res. 62 (1–2), 45–70.

Yin, Y., Xu, X., Wang, D., Yu, Y., Cheng, T., 2024b. Two-stage recoverable robust optimization for an integrated location–allocation and evacuation planning problem. Transp. Res. B Methodol. 182, 102906.

You, F., Grossmann, I.E., 2013. Multicut Benders decomposition algorithm for process supply chain planning under uncertainty. Ann. Oper. Res. 210 (1), 191–211.

Zhang, G., Jia, N., Zhu, N., He, L., Adulyasak, Y., 2023. Humanitarian transportation network design via two-stage distributionally robust optimization. Transp. Res. B Methodol. 176, 102805.

Zhang, T., Wang, S., Xin, X., 2025. Liner fleet deployment and slot allocation problem: a distributionally robust optimization model with joint chance constraints. Transp. Res. B Methodol. 197, 103236.